

National Technical University of Athens

School of Applied Mathematical and Physical Sciences



Postgraduate Studies MSc Program in **Mathematical Modeling
in Modern Technologies and Financial Engineering**

MSc Dissertation on

«**TIME SERIES ANALYSIS AND EXTREME VALUE THEORY**»

Author:

Konstantinos Vasilakakis

Supervisor:

Panayotis G. Michaelides

Athens, Greece

June 2025

**Copyright © Konstantinos Vasilakakis, 2025
All rights reserved.**

Copying, storage, and distribution of this work, in whole or in part, for commercial purposes is prohibited. Reproduction, storage, and distribution for non-profit, educational, or research purposes is permitted, provided that the source is cited and this notice is preserved. Inquiries regarding the use of this work for commercial purposes should be directed to the author.

Acknowledgements

First and foremost, I am deeply grateful to my family for their unwavering support, patience, and understanding during this demanding period. Their encouragement was a constant source of strength and motivation.

I would also like to thank the academic staff for their valuable guidance, availability, and for creating a learning environment that fostered both personal and professional growth.

A special thank you goes to my thesis supervisor, Prof. Dr. Panayotis G. Michaelides, for his insightful feedback, constructive criticism, and continuous support throughout the development of this work. His expertise and encouragement were instrumental in shaping the outcome of this thesis.

To all who stood by me on this journey, thank you!

| | | |
|-------|--|-----------|
| 1. | INTRODUCTION | 7 |
| 2. | METHODOLOGY..... | 11 |
| 2.1 | ARMA MODEL | 11 |
| 2.2 | UNIVARIATE GARCH MODELS | 11 |
| 2.2.1 | Univariate eGARCH | 11 |
| 2.2.2 | Univariate GJR-GARCH | 12 |
| 2.2.4 | Model Selection | 12 |
| 2.3 | DCC-GARCH t-Copula | 13 |
| 2.3.1 | DCC-GARCH conditional correlation matrix | 13 |
| 2.3.2 | DCC-GARCH copula | 13 |
| 2.3.3 | Portfolio weights | 14 |
| 2.4 | QVAR Connectedness Approach | 14 |
| 2.5 | Extreme Value Theory | 15 |
| | Value At Risk | 16 |
| 3. | DATA | 17 |
| 3.1 | Period of study | 17 |
| 3.2 | Data | 17 |
| 4. | EMPIRICAL RESULTS..... | 19 |
| | Summary statistics | 19 |
| | Kendall correlation Matrix | 21 |
| 4.1 | Univariate ARMA fit | 22 |
| 4.2 | DCC-GARCH fit | 24 |
| 4.3 | QVAR Connectedness | 26 |
| | Total Connectedness Index | 26 |
| | Net Connectedness | 27 |
| | Net Directional Connectedness..... | 29 |
| 4.4 | Extreme Value Theory | 30 |
| | Upper Quantile..... | 30 |
| | Lower Quantile..... | 30 |
| | Vine Copula | 31 |
| | Goodness of Fit | 32 |
| | R-Vine Tree Structure..... | 32 |
| | Value at Risk..... | 34 |
| | Portfolio Weights | 34 |
| | Portfolio Value at Risk..... | 35 |

| | |
|---|-----------|
| 5. CONCLUSION | 36 |
| REFERENCES | 38 |
| APPENDIX | 41 |
| Data Plots | 41 |
| Return Plots..... | 41 |
| Summary Statistics | 42 |
| QVAR Connectedness | 42 |
| Total connectedness FROM/TO tables..... | 42 |
| QVAR Directional Connectedness (FROM) | 46 |
| QVAR Directional Connectedness (TO) | 50 |
| QVAR Total Connectedness Index Plot | 55 |
| QVAR Net Connectedness Plot..... | 57 |
| QVAR Connectedness Heatmap Plot..... | 59 |
| QVAR Network Plot | 60 |
| Extreme Value Theory..... | 62 |
| Summary Statistics of empirical returns | 62 |
| Summary Statistics of empirical residuals..... | 62 |
| R-Vine Bivariate Copulas | 63 |
| R-Vine Structure Plots | 63 |
| Plots for minimum variance portfolio weights..... | 66 |
| Plots for minimum correlation portfolio weights | 67 |

ABSTRACT

Periods of heightened financial stress are characterized by uncertainty, abnormally high market volatility, skewed returns and extreme breakdowns in historical asset correlations, which pose significant threats to investment performance and financial stability. This paper discusses the nature of major financial ETFs in stress periods, with a focus on risk, volatility, and tail event dynamics by combining time series econometric models and extreme value theory (EVT), key market sectors and instruments during severe financial crises, such as the 2020 COVID-19 pandemic, geopolitical and banking sector shocks in the early 2020s, and the ongoing inflation-driven tightening cycle.

The time series analysis employs QVAR connectedness approach, ARMA and DCC-GARCH copula models to model and predict leverage effects and volatility clustering, while EVT and R-Vine copulas are employed to model extreme losses, upper and lower tail dependences, and estimate Value at Risk during stressful market periods. We find that asset return distributions are strongly non-normal and fat-tailed in times of crisis, and are characterized by complex dependence structures across the world's largest markets.

Moreover, we show that asset volatility spillovers increase during periods of market stress, which diminishes diversification benefits and increases systemic risk. The research contributes to improving the understanding of financial contagion, tail risk behavior and inter-asset dependencies during periods of increased market tension.

1. INTRODUCTION

The post-2020 era has been mostly characterized by a series of record-breaking disruptions in the global financial system, stretching traditional financial modeling strategies to their limits and exposing underlying vulnerabilities in risk management paradigms. The COVID-19 upheaval created an abrupt reversal of economic activity, then governments and central banks stepped in to deliver monetary easing, fiscal stimuli, debt relief, sectoral assistance, health policies, and external financial assistance to shore up economies and promote healing, ushering in an era of outlier volatility. Constant persistent inflation pressures, central bank monetary tightening, and sectoral breakdowns, such as Silicon Valley Bank collapse, challenged investor confidence and rattled equity and bond markets.

In this span, the financial landscape was reshaped and the understanding of price dynamics during times of heightened stress was in high demand. The Financial Times reported that Silicon Valley Bank's collapse in 2023 was a stark reminder of the fragility of special-purpose financial institutions in the face of tightening monetary settings, triggering widespread volatility and repricing across risk-sensitive assets.

Such crises highlighted the shortcomings of conventional risk modeling methodologies founded on static correlations and simplistic assumptions about market dynamics. Research conducted by Haluszczynski et al. (2019) illustrates that during times of financial turmoil, nonlinear interdependences among assets are strengthened, while linear specifications are inadequate to capture real market processes. Likewise, Liang et al. (2023) illustrate that monetary policy uncertainty and financial stress are asymmetric and interact in a time-varyingly manner. Especially for the situation of non-linear interdependence, time-varying volatility, and fat-tailed distributions, the above limitations have urged researchers as well as investors to use more sophisticated econometric techniques. Studies by Xiong and Idzorek (2011), Eom et al. (2019), and Baur and Lucey (2010) point out that during such periods, returns exhibit steep fat tails, increased skewness, and extreme deviation from normality, implying a higher likelihood of extreme occurrences. Furthermore, the patterns of asset return dependencies also alter significantly.

Samitas, Kenourgios, & Paltalidis (2007), Sokolinskiy (2020), and Trung Hai Le et al. (2021) point out that the interdependence among international stock markets rises in times of crisis. Jajuga, Papla, and Ślepaczuk (2013) call it the phenomenon by which correlations turn into risk factors that are being priced when markets fall, showing their growing significance to portfolio management and risk forecasting. Taken together, literature points to the need for models that transcend static correlation and encompass the dynamic, nonlinear, and often discontinuous co-movements that occur during turbulent times.

Autoregressive-Moving Average (ARMA) models (Peter Whittle 1950, Box and Jenkins 1970), one of the cornerstones of time series analysis, have been broadly used to

model univariate financial series of returns. While used extensively, ARMA models alone fail to capture volatility clustering, a typical feature of asset return series, according to Engle (1982), Bollerslev (1986) and more. This realization leads researchers to resort to more sophisticated GARCH-based models. Engle's (2002) Dynamic Conditional Correlation (DCC-GARCH) model generalizes Bollerslev's (1990) Constant Conditional Correlation (CCC-GARCH) model by allowing correlations between asset returns to be time-varying. While DCC-GARCH models are widely used to predict univariate conditional volatilities and dynamic correlations, most implementations do not capture tail dependences in asset return and volatility distributions.

As a response to the deficiencies of classical correlation-based models, copula-based DCC-GARCH has gained very significant popularity in financial econometrics. Copulas enable flexible joint distribution and dependence structure estimation between various financial instruments, particularly in the tails of the distribution where extreme co-movements are most probable (Patton, 2006). Christensen and Podolskij (2012), applied a Gaussian DCC-GARCH copula model to high-frequency financial data to estimate time-varying dependencies between asset returns with a view to capturing such time-varying dependencies. Their findings support the dynamic behavior of correlations, particularly intraday, where dependence strength increases during the trading day. However, Gaussian copula allows modeling linear dependence relationships between assets, but fail to capture higher tail dependence. Berg and De Smedt (2014) showed that the t-Student copula is particularly more effective for capturing tail dependence compared to the Gaussian counterpart, which fails to account for the joint occurrence of extreme events.

On the other hand, Extreme Value Theory (EVT) has emerged as a robust technique applied to describe the tail of financial return distributions. EVT concerns the tail behavior of the extreme quantiles of a distribution, and provides an estimation technique for Value-at-Risk (VaR) in extreme market states. While EVT has been used in the literature to analyze tail risk within specific time ranges of crisis, the literature is predominantly still univariate in investigating the distribution of asset returns and pays little attention to the complex interdependence of assets and systemic risk in extreme conditions (McNeil et al., 2005).

Recently, the literature has also investigated R-vine copula models owing to their ability to model high-dimensional dependency in a flexible manner as well as for providing a more sophisticated analysis of multivariate risk. R-vine copulas allow multivariate dependence structure to be broken down into a series of pair-copula models, and therefore being flexible and computationally tractable with respect to the traditional multivariate copulas (Aas et al., 2009). Koliai (2016) applies pair-copula construction and EVT to model joint tail risks and stress financial systems, thus reducing complex dependencies to simpler components. Similarly, Paul & Sharma (2017) enhance univariate tail risk forecasting with EVT and eGARCH, by utilizing R-vine copulas in order to integrate multivariate dependence into univariate scenarios.

The authors underscore the significance of models that not only forecast portfolio risk but also capture joint tail dependence and dynamics of several financial assets, as made possible by the R-vine approach.

Parallel to this, literature has also led researchers to focus on the transmission of spillovers through financial systems over a period of time and how the dynamics of time and direction interdependencies are to be taken into account. Particularly, the connectedness approach by Diebold and Yilmaz (2009, 2012), provides a formal framework to capture and represent transmission of shocks between institutions or markets. Their approach presumes application of generalized forecast error variance decompositions (GFEVDs) within a vector autoregressive (VAR) setting to calculate the share of a variable's forecast error variance explained by innovations in other variables. It enables estimation of dynamic, ordering-invariant, directional spillover networks and total and directional connectedness measures. Therefore, it enables full comprehension of systemic connections and their cumulative effects, delivering informative insights in risk surveillance, stress testing, and macroprudential policy implementation.

Moreover, Diebold and Yilmaz (2014) extend their approach to include time-varying connectedness so that dynamic analysis of the evolution of systemic risk across different market regimes is possible. By computing the connectedness measures using a rolling window, their method dissects variations in the size and direction of spillovers, particularly when markets are in stress or turmoil. Most importantly, the resulting system of linkages can be viewed as a dynamic network where variables are nodes and spillovers are edges, allowing us to examine key network measures such as centrality, influence, and fragility. The network perspective delivers new understanding on the structure and propagation of financial shocks and helpful tools for screening systemically important assets or institutions. Nevertheless, apart from all such innovations, their approach operates under a mean-based VAR framework that may not be able to quantify extreme nonlinearities and tail behaviors during periods of financial stress.

In an attempt to close this gap, Ando et. al. (2018) proposed using the Quantile Vector Autoregression (QVAR) model for the investigation of spillovers across different parts of the conditional distribution. Compared to the standard VAR models, the QVAR method estimates dependence patterns at various quantiles, thereby allowing scholars to not only observe how shocks propagate around the mean, but also analyze the transmission mechanism under extreme (lower or upper) market states. This renders the connectedness approach founded on QVAR highly insightful to financial stress testing since it derives quantile-specific spillover channels and network properties involved during times of recession or boom. Nerantzidis, Stoupos, and Tzeremes (2024) showed that volatility spillovers among leading European currencies vary significantly across different market conditions, with stronger connectedness during extreme events.

Altinkeski et. al. (2024) investigated how the VIX index, as a measure of market fear, affects global stock market returns across different market conditions. The study, using a quantile connectedness approach, showed spillovers from the VIX to stock returns are highly asymmetric. The most intense risk transmission occurs during extreme market stress, highlighting that fear contagion intensifies in bear markets. Such findings imply considering asymmetric risk dynamics for better portfolio diversification and risk management in turbulent periods.

Although each of these models has its own strengths, their sole use is common, and such prior study has combined QVAR connectedness, DCC-GARCH, copula-GARCH, EVT, and R-vine copulas in an inclusive framework to investigate financial risk in times of crisis. By utilizing these models separately, the literature lacks their complementary power. The absence of such hybrid models produces a huge gap in the literature, especially during the post-2020 era, where interaction between volatility, tail risk, and interconnectedness is more diversified than ever.

This research tries to bridge the gap by integrating time-series econometrics, extreme value theory, and copula models to have a more comprehensive analysis of general financial risk in times of market stress events. We employ the DCC-GARCH model to account for dynamic correlations and time-varying volatility across asset classes and extend the model using copula-based extensions in order to account for non-linear dependence structures in the tails of the distribution. We also employ R-vine copula models and EVT to account for high-dimensional dependencies and estimate the tail risk measures among groups of multiple assets in financial stress.

By integrating all these different methods, this paper makes two important contributions. First, it highlights the capability of each model to represent such important features of financial stress as volatility clustering, tail risk, and cross-asset dependence. Second, the analysis of specific financial instruments tied to broad equity indices reveals the structure and behavior of the U.S. economy. Broad market indicators tend to reflect the direct effect of systemic shocks, registering across-the-board decreases in investor sentiment and corporate earnings expectations. Their direction warns of contraction or instability on the broader economic horizon and can portend deeper weaknesses in the economic base. Understanding how different market gauges reflect the U.S. economy under stress serves stakeholders well, mainly investors, especially during times of extended uncertainty. It facilitates better decision-making by putting in perspective how different sectors respond to economic shocks, allowing investors to anticipate and not just respond to the movement of the markets when poor timing can spell massive losses. Furthermore, considering that the health of the U.S. economy will have global ramifications, analysis based on these indicators can help international and domestic investors minimize risk exposure.

The rest of the paper is organized in the following way: Section 2 provides a literature review and the paper's methodology. Section 3 presents the data and the most significant crisis episodes which were examined in this research. Section 4 presents the empirical results, in which the relative performance of the models to explain the

financial stress dynamics is emphasized. Lastly, Section 5 concludes the paper by discussing the empirical consequences of our results for risk control and financial regulation.

2. METHODOLOGY

This study employs a combination of advanced econometric and statistical models for estimation of financial time series data. From the integration of ARMA and univariate GARCH models, we determine both the dynamic patterns and volatility clustering in an individual series. To analyze complex tail dependencies and co-movements among related multiple assets, we employ DCC-GARCH t-copulas. Systemic risk and shock transmission analysis is supplemented further by QVAR connectedness that targets volatility spillovers metrics across various quantiles. Finally, Extreme Value Theory and vine copula dependence is subsequently applied to formally examine the dynamics of rare, extreme events robustly to assess risks. These techniques in total constitute a complete framework for assessing both normal and extreme financial market dynamics.

2.1 ARMA MODEL

In this paper we will utilize an Autoregressive-Moving Average of order (p, q) to model the returns for $j = 1, \dots, d$ series of returns in the form of:

$$x_{t,j} = \mu_j + \sum_{k=1}^p \varphi_{k,j} x_{t-k,j} + \sum_{k=1}^q \theta_{k,j} \varepsilon_{t-k,j} + \varepsilon_{t,j} \quad (2.1)$$

Where μ_j represents the mean, $\varphi_{k,j}, \theta_{k,j}$ are the ARMA coefficients of order p, q , and $\varepsilon_{t,j}$ is error term with standardized residuals $\zeta_{t,j} = \frac{\varepsilon_{t,j}}{\sigma_{t,j}}$. The error terms are student's-t distributed with v_j degrees of freedom.

The volatility dynamics from the ARMA model are then modeled with specific univariate GARCH-type models that capture potential asymmetries or leverage effects in the conditional variance.

2.2 UNIVARIATE GARCH MODELS

2.2.1 Univariate eGARCH

The exponential Generalized Autoregressive Conditional Heteroskedasticity (eGARCH) is employed to account for possible non-linear volatility dynamic. The *eGARCH*(1,1) can be expressed as:

$$\log(\sigma_{j,t}^2) = \omega_j + \alpha_j(|e_{j,t-1}| - E[|e_{j,t-1}|]) + \beta_j \log(\sigma_{j,t-1}^2) + \gamma_{GARCH} e_{j,t-1} \quad (2.2)$$

Where ω_j is the constant term, $\alpha_j, \beta_j, \gamma_j$ are the coefficients of the eGARCH model and $e_{j,t}$ are i.i.d. random variables. Since stressful market periods give disproportionately larger emphasis to negative shocks, eGARCH may be inadequate to account for such asymmetry.

2.2.2 Univariate GJR-GARCH

The Glosten-Jagannathan-Runkle Generalized Autoregressive Conditional Heteroskedasticity (GJR-GARCH), account for such asymmetric effects of negative shocks that have a larger impact on volatility than positive shocks. The GJR-GARCH can be expressed as:

$$\sigma_{j,t}^2 = \omega_j + \beta_j \sigma_{j,t-1}^2 + \alpha_j e_{j,t-1}^2 + \gamma_j e_{j,t-1}^2 \mathbb{I}_{j,t-1} \quad (2.3)$$

Where ω_j is the constant term, $\gamma_j, \beta_j, \alpha_j$ are the model coefficients, and $\mathbb{I}_{j,t-1} = 1$ if the error term $e_{j,t-1}$ at $t - 1$ is negative, and $\mathbb{I}_{j,t-1} = 0$ otherwise.

The choice of shock distribution impacts the estimation of model parameters, the forecasting of volatility, and the risk assessment. For this research we will assess several heavy-tail shock distribution models:

| Distribution Error Model | Tail Behavior | Description |
|---------------------------------------|---------------|--|
| t-Students Distribution | Heavy Tail | Efficiently captures heavy-tailed behaviors |
| Skewed t-Students Distribution | Heavy Tail | Assumes asymmetrical behavior of heavy-tailed data |

2.2.4 Model Selection

To select the optimal univariate GARCH model for our data, select the model with the minimum adjusted version of the Bayesian Information Criteria from Antonakakis, Chatziantoniou & Gabauer (2020) which can be expressed as:

$$BIC^* = \log\left(\frac{T^\tau}{\mathcal{L}^2}\right)$$

Where τ represents the number of misspecification tests referred in Antonakakis, Chatziantoniou & Gabauer (2020) and \mathcal{L} is the maximized likelihood function.

The univariate GARCH models are first applied to each return series individually. The standardized residuals are then inputted into the DCC-GARCH t-copula model, to estimates time-varying correlations between series. This method handles both

dynamic dependence and the heavy tails that are usually encountered in joint financial return distributions.

2.3 DCC-GARCH t-Copula

2.3.1 DCC-GARCH conditional correlation matrix

For a $N \times 1$ vector \mathbf{x}_t of time-series with different marginal distribution of shocks and $\mathbf{z}_t = \mathbf{H}_t^{-1} \mathbf{e}_t$ the standardized residuals vector, the CCC-GARCH estimator of the Bollerslev (1990) is calculated as:

$$\mathbf{B} := \frac{1}{T} \sum_{t=1}^T \mathbf{z}_t \mathbf{z}_t^T \quad (2.4)$$

And \mathbf{H}_t is a diagonal matrix containing the conditional volatilities.

Engle (2002) generalized the Bollerslev approach to account for changes over time in the correlation. The dynamic conditional correlations of a DCC-GARCH(1,1) at time t with GARCH coefficients a, β and unconditional variance-covariance matrix of standardized residuals $\boldsymbol{\rho}$ are calculated as:

$$\boldsymbol{\rho}_t = (1 - a_{DCC} - b_{DCC})\boldsymbol{\rho} + \beta_{DCC}\boldsymbol{\rho}_{t-1} + a_{DCC}\mathbf{z}_t\mathbf{z}_t^T \quad (2.5)$$

2.3.2 DCC-GARCH copula

For the DCC-GARCH dependence structure, any multivariate distribution can be expressed through its marginal distributions using copulas (Sklar, 1959), which describe the dependence structure between the variables. For a vector $Y = (Y_1, \dots, Y_n)$ of random variables with joint distribution function $F(\mathbf{y})$ where $\mathbf{y} = (y_1, \dots, y_n)$, and $F_1(y_1), \dots, F_n(y_n)$ the corresponding marginal distributions of each random variable, a copula function $C(\cdot)$ exists such that:

$$F(\mathbf{y}) = C(F_1(y_1), \dots, F_n(y_n))$$

Patton (2006) extended this approach by introducing time-varying conditional copulas. Utilizing this framework, we can express the multivariate mixed DCC-GARCH t-copula model as follows:

$$C(\mathbf{u}|\mathbf{p}_t, v) = t_v \left(F_{Y_1}^{-1}(u_1|\mathbf{p}_1), \dots, F_{Y_N}^{-1}(u_N|\mathbf{p}_N) \right) \quad (2.6)$$

Where t_v is the c.d.f. of the t-Copula with V degrees of freedom and \mathbf{p}_i are the estimated parameters of each fitted univariate GARCH model. The copula is calculated based on the DCC-GARCH conditional correlations:

$$t_v \left(F_{Y_1}^{-1}(u_1|\mathbf{p}_1), \dots, F_{Y_N}^{-1}(u_N|\mathbf{p}_N) \right) = \int_{-\infty}^{F_{Y_1}^{-1}(u_1|\mathbf{p}_1)} \dots \int_{-\infty}^{F_{Y_N}^{-1}(u_N|\mathbf{p}_N)} \frac{\Gamma\left(\frac{V+N}{2}\right) \left(1 + \frac{1}{V} \boldsymbol{\zeta}_t^T \mathbf{K}_t^{-1} \boldsymbol{\zeta}_t\right)^{\frac{(N+V)}{2}}}{\Gamma\left(\frac{V}{2}\right) |\mathbf{K}_t|^{1/2} (V\pi)^{N/2}}$$

And $\mathbf{K}_t = \text{diag}(\boldsymbol{\rho}_t)^{-\frac{1}{2}} \boldsymbol{\rho}_t \text{diag}(\boldsymbol{\rho}_t)^{-\frac{1}{2}}$.

The outputs of the model are utilized to construct risk minimization portfolio weights in order to construct a general Value at Risk for the studied portfolio.

2.3.3 Portfolio weights

Markowitz, H. (1952) proposed the **Minimum Variance Portfolio (MVP)** construction approach utilizes portfolio variance as a measure of risk to identify asset weights reducing overall portfolio risk. The weights are derived from the conditional variance-covariance matrix $\mathbf{Q}_t = \text{diag}(\boldsymbol{\rho}_t)^{-\frac{1}{2}} \boldsymbol{\rho}_t \text{diag}(\boldsymbol{\rho}_t)^{-\frac{1}{2}}$.

$$w_{R_t}^{MVP} = \frac{\mathbf{Q}_t^{-1} \mathbf{1}}{\mathbf{1} \mathbf{Q}_t^{-1} \mathbf{1}} \quad (2.7)$$

Where $\mathbf{1}$ is a vector of ones.

Minimum Correlation Portfolio (MCP) computes asset weights that reduce the overall correlation among portfolio members to a minimum. The weights are approximated based on the conditional variance-covariance matrix:

$$w_{R_t}^{MCP} = \frac{\left[\text{diag}(\mathbf{Q}_t)^{-\frac{1}{2}} \mathbf{Q}_t^{-1} \text{diag}(\mathbf{Q}_t)^{-\frac{1}{2}} \right]^{-1} \mathbf{1}}{\mathbf{1} \left[\text{diag}(\mathbf{Q}_t)^{-\frac{1}{2}} \mathbf{Q}_t^{-1} \text{diag}(\mathbf{Q}_t)^{-\frac{1}{2}} \right]^{-1} \mathbf{1}} \quad (2.8)$$

2.4 QVAR Connectedness Approach

Building on this, while DCC-GARCH assumes the time-varying nature of asset correlations, QVAR connectedness extends the analysis further by examining how shock transmission changes across the system at different quantiles in the return distribution. This study employs the **Ando et al. (2018)** Quantile Connectedness approach.

The QVAR model for a $N \times 1$ vector of returns x_t can be expressed as:

$$x_t = \mu^{(q)} + \boldsymbol{\Phi}_t^{(q)} x_{t-1} + \varepsilon_t^{(q)} \quad (2.9)$$

Where $\mu^{(q)}$ is the $N \times 1$ vector of the conditional mean $\boldsymbol{\Phi}_t^{(q)}$ is the QVAR coefficient matrix of $N \times N$ dimensions and $\varepsilon_t^{(q)}$ is the $N \times 1$ vector of the error term. The index q denotes the respective quantile which allows the parameters to vary across different quantiles. The respective K-step ahead GFEVD is:

$$\tilde{\psi}_{ij}(K) = \frac{(\boldsymbol{\Sigma}^{(q)})^{-1} \sum_{k=1}^{K-1} \left[\ell_k^T \tilde{\mathbf{B}}_k^{(q)} \boldsymbol{\Sigma}^{(q)} \ell_k \right]^2}{\sum_{k=1}^{K-1} \left(\ell_k^T \tilde{\mathbf{B}}_k^{(q)} \boldsymbol{\Sigma}^{(q)} \left(\tilde{\mathbf{B}}_k^{(q)} \right)^T \ell_k \right)} \quad (2.10)$$

Where $\Sigma^{(q)}$ is the (quantile) variance covariance matrix of $N \times N$ dimensions, ℓ_k is the selection vector and $\tilde{B}_k^{(q)}$ is the Quantile Vector Moving Average (QVMA) representation matrix of coefficients. The normalized K-step GFEVD:

$$\tilde{\psi}_{ij}^*(K) = \frac{\tilde{\psi}_{ij}(K)}{\sum_{j=1}^N \tilde{\psi}_{ij}(K)} \quad (2.11)$$

QVAR Shock Transmissions from variable i to all other variables

$$C_{i \rightarrow j, t}^{QVAR}(K) = 100 \cdot \frac{\sum_{j=1, i \neq j}^N \tilde{\psi}_{ji}^*(K)}{\sum_{j=1}^N \tilde{\psi}_{ji}^*(K)}$$

QVAR Shock Transmissions from all variables (excluding i) to i :

$$C_{i \leftarrow j, t}^{QVAR}(K) = 100 \cdot \frac{\sum_{j=1, i \neq j}^N \tilde{\psi}_{ij}^*(K)}{\sum_{j=1}^N \tilde{\psi}_{ij}^*(K)}$$

QVAR Total connectedness to variable i :

$$C_t^{QVAR}(K) = 100 \cdot \frac{\sum_{i,j=1, i \neq j}^N \tilde{\psi}_{ij}^*(K)}{\sum_{i,j=1}^N \tilde{\psi}_{ij}^*(K)}$$

QVAR Net total directional connectedness

$$C_{i,t}^{QVAR}(K) = C_{i \rightarrow j, t}^{QVAR}(K) - C_{i \leftarrow j, t}^{QVAR}(K)$$

QVAR analyzes how shocks impact a network of time series during extreme market conditions, rendering it ideal in measuring the intensity of tail risk spillovers. QVAR connectedness does not focus on the tail behavior, but emphasizes how extreme shocks propagate across a system of variables. In the next section, Extreme Value Theory and Vine copulas account for the non-linear dependencies and joint tail behavior among the financial variables.

2.5 Extreme Value Theory

For the extreme value analysis, we will utilize the Generalized Pareto Distribution proposed Pickands (1975), to model the residual distribution tails (Koliai, 2016) and transform into uniform margins:

$$F_{emp,j}(res_t) = \begin{cases} k_D GPD_j(-\zeta_t | -q_{emp,j}(a_D), \sigma_{D,j}, \xi_{D,j}), & q_{emp,j}(a_D) \geq \zeta_t \\ g_j(\zeta_{t,j}), & q_{emp,j}(a_D) < \zeta_{t,j} < q_{emp,j}(a_U) \\ 1 - k_U GPD_j(\zeta_t | q_{emp,j}(a_U), \sigma_{U,j}, \xi_{U,j}), & q_{emp,j}(a_U) \leq \zeta_t \end{cases} \quad (2.12)$$

Where k_D, k_U are the proportion of observations that fall below or above the empirical quantile (GPD threshold), $g_j(\cdot)$ is the error distribution of the j^{th} time series,

$q_{emp,j}(a_D), q_{emp,j}(a_U)$ are the upper and lower empirical quantiles - thresholds of the Generalized Pareto Distribution calculated at the a_D, a_U percentiles, and $\sigma_{.j}, \xi_{.j}$ are the respective generalized pareto distribution parameters.

We will use the above distribution at the normalized residuals $\zeta_{t,j}$, to obtain the Probability Integral Transformation of the time series, and simulate K returns at $t + 1$, using a Multivariate R-Vine Copula Dependence Structure:

$$C(F_{emp,1}(\cdot), \dots, F_{emp,N}(\cdot)) = \prod_{h=1}^{N-1} \prod_{(l_1, l_2) \in T_h} \mathcal{B}_{l_1, l_2 | \theta_t}(F_{emp, l_1}(\cdot), F_{emp, l_2}(\cdot) | F_{emp, \theta_t}(\cdot)) \quad (2.13)$$

Where T_j represent the tree that models the pairwise dependence structure between variables, θ_t are the conditioning set of variables in each tree, and $\mathcal{B}_{.|.}$ represent the bivariate conditional copula structure between the margins.

Value At Risk

We will use the above copula dependence structure to simulate $1, \dots, N$ future returns of the portfolio at $t + 1$ by inverting empirical distribution in (2.12), multiplying the empirical errors by the one step ahead prediction of the volatility using the DCC-GARCH model, and using the ARMA(1,1) parameters we create N random vectors of one step ahead returns. Utilizing the weights derived in Sections 2.7 and 2.8, we will compute the value at risk for both tails of the distribution for the minimum variance and minimum correlation portfolios as follows:

Minimum Variance Portfolio - VaR

$$VaR_D^{mvp}(a_D) = \sum_{j=1}^N w_j^{mvp} Q_{a_D}(x_{j,t+1})$$

$$VaR_U^{mvp}(a_U) = \sum_{j=1}^N w_j^{mvp} Q_{a_U}(x_{j,t+1})$$

Minimum Correlation Portfolio - VaR

$$VaR_D^{mcp}(a_D) = \sum_{j=1}^N w_j^{mcp} Q_{a_D}(x_{j,t+1})$$

$$VaR_U^{mcp}(a_U) = \sum_{j=1}^N w_j^{mcp} Q_{a_U}(x_{j,t+1})$$

$Q_p(\cdot)$ denotes the empirical quantile function evaluated at the levels a_D, a_U .

3. DATA

3.1 Period of study

Studying returns during upheaval times is significant for understanding market during extraordinary events where risk and volatility are heightened. Asset prices often fluctuate, and investor sentiment can reverse abruptly. Furthermore, it has been observed in multiple studies in the literature that there is a tendency for asset correlations to change, making typical diversification strategies less efficient. Identifying sectors that are more likely to be resilient or poised to recover is crucial, in order for investors to be able to rework their investments appropriately.

The importance of studying asset behavior amidst crisis has significantly increased after 2020 because the global financial system has faced a succession of disrupter events whose effects go beyond the direct consequences of COVID-19. The market fluctuation caused by the pandemic brought out the vulnerabilities of the markets, with large-scale infusions of liquidity, interest rate cuts, and fiscal stimuli affecting the asset prices in ways that ran against standard models. With correlations across various asset classes increasing, the pandemic reminded us of the importance of knowing return behavior during times of extreme stress.

In the aftermath of the COVID-19 pandemic, financial markets continued to be beset by the after-effects of the crises. The Russia-Ukraine war in 2022 caused enormous volatility in energy prices, created supply chain disruptions, and heightened geopolitical tensions, all of which significantly affected global equity, bond, and commodity markets. Consequently, rates of inflation increased to record levels in many developed economies, forcing central bank authorities like the Federal Reserve and the European Central Bank to adopt sharp monetary tightening policies. These hikes in interest rates increased market volatility, value declines in bonds, and a reallocation of risk in investment portfolios.

In recent times, the banking industry faced new challenges in 2023 after the collapses of institutions like Silicon Valley Bank and Credit Suisse, which once again raised alarms over financial stability. These events caused abrupt changes in investors' perceptions, increased credit risk, and led to material shifts within the bank industry.

3.2 Data

The SPDR S&P 500 ETF Trust (SPY) is one of the most prominent and widely traded exchange-traded funds in the world. Its primary objective is to track the performance of the S&P 500 Index, an index of 500 of the largest publicly traded firms in the US. Accordingly, while SPY is a popular core holding for both institutional and individual investors seeking diversification and long-term capital growth. Its low expense ratio and high liquidity only serve to enhance its appeal as a core investment product.

The ProShares VIX Short-Term Futures ETF (VIXY) tracks the S&P 500 VIX Short-Term Futures Index which is based on the CBOE Volatility Index (VIX), an index of expected market volatility. The ETF is almost exclusively used as a hedge or for short-term trading during periods of anticipated market volatility. But due to the nature of futures contracts and a phenomenon known as "contango," VIXY inevitably loses value over time and is unsuitable for long-term investors.

The Vanguard Real Estate ETF (VNQ) gives investors targeted exposure to the U.S. real estate market by tracking an index of real estate investment trusts (REITs). The REITs in question primarily own and operate income-producing properties such as office buildings, shopping centers, and apartment complexes. VNQ is popular with investors seeking high dividend yields and diversification outside of traditional stocks and bonds. Its fortunes, though, are tied directly to the health of the real estate industry and are rate-sensitive to interest rate movements, which impact property values and borrowing costs.

The Financial Select Sector SPDR Fund (XLF) tracks a wide range of financial institutions including banks, insurers, and investment companies. XLF exposes to financial services that can benefit them from accelerating economic growth and rising interest rates. Its low operating expense ratio and presence of the banking giants like JPMorgan Chase and Berkshire Hathaway have turned it into a favorite for those who want to cash in on trends in the banking industry. Yet, due to its inherent characteristics, it remains vulnerable to industry-specific risks like regulatory reform and economic collapses.

Finally, the Materials Select Sector SPDR Fund (XLB) targets the materials sector, such as producers of chemicals, metals, mining, paper, and construction materials. XLB is a cyclical investment that performs well when the economy is expanding and demand for raw materials is high. This ETF offers investors a chance to invest in the underlying industries that drive economic growth, but its performance can be volatile because it closely follows commodity prices and global economic activity.

During the study period, the behavior of these ETFs becomes highly interdependent and sensitive and tend to plummet steeply and become highly correlated when investors shed risk assets uniformly, compounding losses across sectors. VIXY, however, tends to spike when volatility in the market is at its peak, with transient hedging utility but with value erosion when the holding period is prolonged. Industry-focused ETFs like VNQ and XLF are most vulnerable to crises in their sector, the real estate and financial sectors normally suffering in a credit or liquidity crisis. Most often, crises raise connectedness and volatility within these funds, lowering the functionality of diversification across portfolios and exposing investors to lower drawdowns and more systemic risk.

4. EMPIRICAL RESULTS

Summary statistics

| | SPY | VIXY | VNQ | XLF | XLB |
|--------------------|-----------------|-------------|------------|-----------------|-----------------|
| Mean | 0 | -0.001 | 0 | 0 | 0 |
| (p-value) | 0.173 | 0.421 | 0.8 | 0.285 | 0.371 |
| Variance | 0 | 0.002 | 0 | 0 | 0 |
| Skewness | -0.531*** | 2.095*** | -1.100*** | -0.175*** | -0.280*** |
| (p-value) | 0 | 0 | 0 | -0.01 | 0 |
| Ex.Kurtosis | 11.201*** | 11.946*** | 17.228*** | 13.780*** | 9.227*** |
| (p-value) | 0 | 0 | 0 | 0 | 0 |
| JB | 6941.770*** | 8786.808*** | 16540.6*** | 10418.68*** | 4685.429*** |
| (p-value) | 0 | 0 | 0 | 0 | 0 |
| ERS | -8.682*** | -6.019*** | -12.121*** | -8.262*** | -5.571*** |
| (p-value) | 0 | 0 | 0 | 0 | 0 |
| Q(20) | 164.610*** | 18.560** | 86.997*** | 155.965*** | 121.496*** |
| (p-value) | 0 | -0.032 | 0 | 0 | 0 |
| Q2(20) | 1749.398** * | 210.240*** | 931.871*** | 1620.082** * | 1442.693** * |
| (p-value) | 0 | 0 | 0 | 0 | 0 |

Table 2: ¹Summary Statistics of the Variables

The remarkably high pvalue of the mean of all returns series indicates no statistically significant deviation from zero. This is a prevalent indicator of an efficient market behavior, where the daily returns are expected to fluctuate around zero in the absence of foresight patterns.

Return distributions of all ETFs are strongly non-normal, evidenced by high levels of skewness and excess kurtosis. SPY, VNQ, XLF, and XLB's negative skewness means that these funds have larger extreme negative returns than positive ones. This indicates increased market stress and downside risk. On the contrary, VIXY's high positive skewness implies large positive jumps in volatility, suggesting spikes in market stress and investors' fear or risk aversion. Extreme excess kurtosis for all ETFs confirms the existence of fat tails, meaning extreme return results are more likely than in a normal distribution. Strongly evidenced against normality by the Jarque-Bera test, where all p-values at the 1% level of significance reject the null hypothesis of normality.

1) ***, **, and * indicate the significance levels at the 1%, 5%, and 10% respectively. Skewness is evaluated using the method proposed by D'Agostino (1970), while kurtosis is determined based on the Anscombe and Glynn (1983) approach. The Jarque-Bera (1980) test provides the JB statistic to assess normality. ERS denotes the unit root test developed by Elliott, Rothenberg, and Stock (1996). The Q²(20) statistic represents the weighted Portmanteau test for residual autocorrelation, as introduced by Fisher and Gallagher (2012).

The ERS unit root test confirms the stationarity of each return series at a 1% significance level. Return shocks are fleeting and return series revert to a stable mean over time. The stationarity of our time series is crucial, since the selected models of this paper function properly under the hypothesis of stationarity.

The discovery of high serial correlation, as evidenced by the Ljung-Box Q-statistics at lag 20, suggests that past returns contain information about future returns, especially at short horizons. In addition, the extremely high Q^2 statistics provide very strong evidence of volatility clustering, a ubiquitous feature of financial time series in which large changes in the return are followed by further large changes (of opposite sign), and small changes are followed by small changes. This indicates non-stability of volatility over time and favors the use of models that can handle time-varying volatility dynamics.

In summary, the statistical profile of such ETFs features characteristics typical with financial markets: no serial return drift, asymmetric and non-normal return distributions, serial dependence, and conditional heteroskedasticity—all features which are worth keeping in mind when dealing with risk management, portfolio allocation, and econometric modeling.

Kendall correlation Matrix

| | SPY | VIXY | VNQ | XLF | XLB |
|-------------|------------|-------------|------------|------------|------------|
| SPY | 1.000*** | -0.557*** | 0.504*** | 0.567*** | 0.576*** |
| VIXY | -0.557*** | 1.000*** | -0.357*** | -0.426*** | -0.433*** |
| VNQ | 0.504*** | -0.357*** | 1.000*** | 0.461*** | 0.476*** |
| XLF | 0.567*** | -0.426*** | 0.461*** | 1.000*** | 0.588*** |
| XLB | 0.576*** | -0.433*** | 0.476*** | 0.588*** | 1.000*** |

Table 3: Kendall Correlation Matrix

The Kendall rank correlation matrix reveals statistically significant monotonic relations in all ETF pairs and identifies strong co-movements in ordinal return patterns. SPY, XLF, and XLB have the highest positive correlations with a correlation coefficient of over 0.56. This suggests U.S. large-cap equities (SPY), financials (XLF), and materials (XLB) tend to move together in rank order, which is evidence of similar underlying drivers such as growth expectations, monetary policy, and investor sentiment.

VNQ (Real Estate) is also moderately to strongly positively correlated with SPY (0.504***) and XLF (0.461***), suggesting real estate returns move in tandem with the broader equities and the financial sector, respectively, since they share their responsiveness to interest rates and the cycle.

VIXY, being short-term volatility futures, has consistently negative correlations with all other ETFs but most prominently with SPY (-0.557***). This is anticipated as VIXY typically rises in equity market downturns. Its negative correlation with VNQ, XLF, and XLB also confirms its role as a counter-cyclical hedge during periods of market distress.

The repeatedly significant magnitude throughout all correlations affirms the robustness of these rank-based relationships. As Kendall's tau is a nonparametric measure, these results will also be applicable when there is non-normality or extremes in outliers—a common feature of financial return information.

The significant positive correlations between SPY, XLF, and XLB imply little diversification potential within U.S. cyclical groups, while the negative correlation between VIXY and equity-based ETFs suggest that it can be utilized as a volatility hedge.

4.1 Univariate ARMA fit

| | Parameter | Estimate | Std. Error | t-value | p-value |
|------|-----------|-----------|------------|-----------|-------------|
| SPY | μ_1 | 0.000793 | 0.000212 | 3.7383 | 0.000185*** |
| | AR | 0.672673 | 0.062519 | 10.7595 | 0*** |
| | MA | -0.693454 | 0.060751 | -11.4148 | 0*** |
| VIXY | μ_2 | -0.00478 | 0.000488 | -9.7955 | 0*** |
| | ar1 | 0.92109 | 0.012007 | 76.7127 | 0*** |
| | ma1 | -0.95747 | 0.003651 | -262.2432 | 0*** |
| VNQ | μ_3 | 0.000363 | 0.000295 | 1.2286 | 0.219238 |
| | ar1 | -0.841475 | 0.329203 | -2.5561 | 0.010585** |
| | ma1 | 0.852763 | 0.318114 | 2.6807 | 0.007347*** |
| XLF | μ_4 | 0.000548 | 0.000297 | 1.8474 | 0.064694 |
| | ar1 | -0.968737 | 0.005855 | -165.4523 | 0*** |
| | ma1 | 0.979893 | 0.000467 | 2098.8664 | 0*** |
| XLB | μ_5 | 0.000108 | 0.0003 | 0.359 | 0.719599 |
| | ar1 | -0.857538 | 0.087965 | -9.7486 | 0*** |
| | ma1 | 0.875134 | 0.081811 | 10.6971 | 0*** |

Table 4: Univariate ARMA fit

The ARMA (1,1) model was chosen for all ETFs based on both theoretical parsimony and empirical diagnostic performance. The criterion used in validating model adequacy is the Weighted Ljung-Box test (WLB test), and targets the lag lengths recommended by Tsay (2010), as $2(p + q) + (p + q) - 1 = 5$ and $2(p + q) + (p + q) - 1 = 9$. The results below support the adequacy of orders $p = q = 1$ for each asset:

| | Lag[5] | | Lag [9] | |
|------|------------|---------|------------|---------|
| | statistics | p-value | statistics | p-value |
| SPY | 0.88243 | 1.0000 | 3.06076 | 0.8812 |
| VIXY | 0.2403 | 1.0000 | 0.8122 | 0.9999 |
| VNQ | 0.45651 | 1.0000 | 1.21139 | 0.9992 |
| XLF | 1.94035 | 0.6326 | 2.66319 | 0.8130 |
| XLB | 1.48949 | 0.9981 | 4.55260 | 0.5586 |

Table 5: ARMA lag selection

The ARMA estimation results for each of the five series indicate strong short-run relationships in returns. All of the five series have significant autoregressive (AR) and/or moving average (MA) parameters, indicating deviations from white noise and highlighting serial correlation structures characteristic of financial time series.

A persistent ARMA(1,1) pattern is seen, while the form and magnitude of the parameters are different. Some have positive AR coefficients and negative MA terms reflecting moderate momentum followed by immediate reversal. Others consist of large negative AR terms and positive MA terms, reflecting strong mean-reversion tendencies where returns get corrected sharply after drift—behavior consistent with rapid price correction to new information. Notably, one of the series has almost ± 1 AR and MA coefficients, which suggests extremely persistent dynamics and good shock absorption, and suggests that return innovations are large and long before being absorbed.

This high persistence underscores the importance of considering such effects when modeling volatility and predicting returns. Another set has a negative AR coefficient and a positive MA coefficient but lower magnitudes and borderline significance. This setup indicates shocks to be smoothed instead of reversed immediately, in line with a delayed adjustment mechanism in return behavior. In general, the ARMA(1,1) specification is a good fit for both series, describing the time dependence in a concise way. The choice is also corroborated by residual diagnostic tests (e.g., Weighted Ljung-Box), which confirm no appreciable residual autocorrelation remaining and validate the model form and presence of exploitable serial dependencies observed, which can be utilized to inform forecasting models and short-horizon trading models.

4.2 DCC-GARCH fit

In the table below, the coefficients of the DCC-GARCH estimated model:

| Parameter | SPY | VIXY | VNQ | XLF | XLB |
|------------------------------|--------------------------------|--------------------------------|--------------------------------|--------------------------------|--------------------------------|
| GARCH type | eGARCH | eGARCH | gjr-GARCH | eGARCH | eGARCH |
| (criterion) | -8369.106 | -4978.496 | -7795.782 | -7857.022 | -7870.244 |
| (SB) | 0.1805898 | 0.3123912 | 0.100856 | 0.6799576 | 0.185704 |
| (W20) | 0.8751058 | 0.9790883 | 0.7559414 | 0.8028572 | 0.1733706 |
| (VaR) | 0.1050806 | 0.5988842 | 0.4395479 | 0.9192488 | 0.6275906 |
| (CVaR) | 0.1340 | 0.9680 | 0.1130 | 0.658 | 0.2390 |
| (VaR Dur) | 0.2769508 | 0.495891 | 0.2053008 | 0.3991534 | 0.1645124 |
| μ (pvalue) | 0.000732 (0.000383) | 0.000040 (0.972698) | 0.000157 (0.609479) | 0.000404 (0.209446) | 0.000116 (0.701358) |
| ω (pvalue) | -0.244589 (0.000000) | -0.562584 (0.000133) | 0.000005 (0.002627) | -0.243264 (0.000000) | -0.126319 (0.000000) |
| β (pvalue) | 0.973945 (0.000000) | 0.910029 (0.000000) | 0.898108 (0.000000) | 0.972271 (0.000000) | 0.985647 (0.000000) |
| γ (pvalue) | 0.139424 (0.000000) | 0.189026 (0.000003) | 0.120712 (0.000002) | 0.194197 (0.000069) | 0.120124 (0.000000) |
| ARCH (pvalue) | -0.163812 (0.000000) | 0.224646 (0.000000) | -0.012904 (0.303287) | -0.125884 (0.000000) | -0.089029 (0.000000) |
| <i>Residual Distribution</i> | Students-t | Skewed-t | Skewed-t | Skewed-t | Students-t |
| D.F. (pvalue) | 7.312277 (0.000005) | 4.517621 (0.000000) | 7.292060 (0.000000) | 9.508247 (0.000809) | 13.262886 (0.001506) |
| ξ (pvalue) | – | 1.657962 (0.000000) | 0.912440 (0.000000) | 0.900379 (0.000000) | – |

Table 6: ¹DCC-GARCH estimates

The DCC-GARCH estimates $a_{DCC} = 0.038067$ ($pvalue = 0.000000$) and $b_{DCC} = 0.931972$ ($pvalue = 0.000000$), suggest high persistence in conditional correlations and extreme volatility clustering, which both support the evidence that the co-movement among the assets responds moderately to recent shocks but maintains high memory through time. Persistence of volatility remains high throughout this research, which shows that uncertainty among investors is not temporary and markets continue to digest the impact of shocks over an extended period of time.

1) SB refers to **Sign Bias Test** (Engle & Ng, 1993) that tests for **asymmetric effects** of positive and negative shocks on volatility. W20 refers to **WARCH (20) Tests** (Engle & Ng, 1993) that detects ARCH effects within the range of 20 lags. VaR, CVaR represent Value at Risk & Conditional Value at Risk, and VaR Dur checks if violations are randomly spaced.

Furthermore, the estimated t-copula shape parameter $V = 11.368733$, ($pvalue = 0.000000$), shows the ETF returns have moderate tail dependence. The results from all the statistical tests and the DCC-GARCH model are all evidence in support of high volatility and statistically significant persistence of volatility.

The extremely strong asymmetric reaction to shocks of XLF and VIXY shows that negative news have disproportionately larger effect on volatility than positive news. Further, the ARCH coefficient in VIXY is significantly higher than in other assets, which leads to excessive responsiveness under market uncertainty. As XLF represents the financial sector, its high asymmetric volatility shock response and VIXY's volatility persistence indicate that bad news can exacerbate economic downturns much more and for longer periods than other sectors. Hence, forecasting and risk management must be calibrated to the financial sector's sensitivity to market stress.

The distributional characteristics of returns, which are derived with Student's t and Skewed-t distributions, indicate fat tails and statistically significant skewness in VIXY, VNQ and XLF. Fat tails indicate that extreme events in markets have greater probabilities of occurrence, confirming experience in the past under crises as asset prices drop rapidly and sharply. VIXY has the highest positive skew ($\xi_{VIXY} = 1.657962$) and heavier tail ($df_{VIXY} = 4.517621$), meaning that volatility products that are able to notice sudden, large rises in value whenever fear in the market is created. VNQ and XLF also show a pattern for large positive returns to be more common or larger than for large negative returns. More broadly, the results reveal non-linear highly networked and responsive contemporary financial markets. For the broader economy, this implies increased systemic risk, unbalanced market reaction, and significant vulnerabilities transmitted from one market sector to another. For policymakers, the message is regulators and central banks must be vigilant. In order to avoid unintended market reaction, communication needs to be transparent, calibrated, and timely, and policy action on the basis of careful consideration of cross-sector sensitivities and market sentiments.

4.3 QVAR Connectedness

Total Connectedness Index

Figures 24 to 32 represent the Total Connectedness index ranging within 10% to 90% QVAR quantile and finally Figure 42 is the heatmap of the total connectedness index.

For this paper, the rolling window value is set to be 100. The overall connectedness is noticeably high for the lower quantiles (10% and 20%) and the higher quantiles (80% and 90%). Particularly, the rise in connectedness at the lower tail is clearly associated with highly publicized episodes of financial strain, such as the COVID-19 crash of March 2020 and the inflation-driven market corrections of 2022. In the upper tail, increased connectedness identifies periods of strong market rebounds or speculative booms such as the strong equity recovery on stimulus during late 2020, and potentially tech-led rallies in 2023 and early 2024. Furthermore, the total connectedness graph shows persistent fluctuation in the index throughout the whole sample period. The latter suggest that the strength of interdependence among assets is time-varying and possibly reflect shifting macroeconomic expectations under uncertain investors' moods and policy statements.

Additional findings in the mid quantiles range show that interconnectedness is lower than the tails, but was persistently high from early 2022 to mid-2023. This outcome was unexpected, given that moderate quantiles typically represent standard market conditions. But this level of interconnectivity suggests that the market was structurally stressed. The Russian-Ukrainian war and inflation shocks were undoubtedly significant contributors.

This mid-quantile persistence during this period was not just a transitory shock but rather a structural problem. As such, markets were operating in a high-policy-sensitivity environment, where even normal economic data releases could potentially create broad-based spillovers.

Another major contributor could be the early 2023 banking crisis, linked to Silicon Valley Bank's failure. While this did not produce an excessive tail shock to the whole market, it did generate a high degree of stress in financials and produced more global concerns regarding liquidity and credit risk.

Conversely, tail risk significantly in the tails but more intriguingly, there is strong evidence of persistent connectedness in the middle quantile range of the return distribution in times of policy-induced uncertainty in 2022–2023.

Net Connectedness

Figures 33 to 41 refer to Net Connectedness index is plotted ranging within 10% to 90% QVAR quantile and Figures 43 to 51 illustrate the network plot of connectedness for the aforementioned quantiles.

SPY acts consistently as a net broadcaster of shocks across all quantiles — from periods of deep trough (10% and 20% quantiles), to normal market periods (30% to 70%), up to strong bull periods (80% and 90%). During the first half of the sample period, particularly during 2020-2023, the net connectedness of SPY was particularly elevated. It was a period dominated by regime-level themes such as the COVID-19 pandemic, aggressive monetary policy response, and wild swings in investor sentiment. In such regimes, SPY transmitted a lot of information or volatility to other asset classes since it was the epicenter of the world financial system. It established and controlled the overall market tone, pushing sectors across the board.

Yet, from mid-2023 through mid-2024, the connectedness of SPY was temporarily mildly negative and indicated that its role in driving systemic moves was lessened. This may have been due to relative market tranquility or sector decoupling in which other asset classes or drivers (e.g., commodities or policy surprises) assumed more of a leadership role in risk transmission. By the last sample, SPY's positive connectedness re-emerged, indicating renewed reassertion of its leadership role — perhaps related to heightened macroeconomic uncertainty or reacceleration of U.S. equity performance.

Under mid quantile regimes (30% to 70%), SPY remains a solid propagator of shocks with very high connectedness between 2020 to 2023. This implies that even during moderate stress levels of the market, price movements of SPY are of systemic importance due to its pervasive exposure to all market sectors and as a bellwether of US economic sentiment. For quantiles higher than 80% and 90%, where the returns are strong, SPY holds this transmission function. Bull market rallies in SPY produce spillovers across asset classes, inducing risk-on actions, capital inflows, and cyclical sector rotation. The uniform transmitter behavior of SPY across quantiles is a feature of its structural involvement in financial interconnectedness.

VIXY exhibits a distinctly different behavior compared to other assets. Across nearly every quantile, VIXY is a net recipient of shocks, reflected in a consistently negative connectedness index. As a volatility product, it acts as a responder to market financial stress. For left-tail occurrences (10% and 20% quantiles), VIXY absorbs shocks from the overall market, often spiking to declines in SPY and other risk assets. Additionally, there are fleeting times — most notably between late 2021 and early 2022, and then between mid-2023 and mid-2024 — when VIXY's connectivity goes positive, suggesting that volatility itself had become an agent of systemic influence. These periods overlap with policy surprises, inflation fears, or geopolitical crises driving volatility upward and creating spillovers in asset markets.

In mid quantiles, VIXY continues to be a net receiver, except for the positively connectedness period near the 50% quantile during mid-2021 to mid-2022. This is consistent with a high but not exceptionally high volatility regime, in which volatility levels may have influenced risk positioning and asset repricing, but perhaps not necessarily crisis on a linear basis. In upper quantiles, VIXY continues to act as a shock absorber, with extremely violent fluctuations in its connectedness index. Even during bull markets, volatility will occasionally spike as a function of event risks or technical considerations. But these spikes are typically reactive, as opposed to driving the overall market action.

XLF (Financials) is generally a net transmitter of shocks in general, especially in low and high quantile environments, affirming its systemic importance. In the 10% and 20% quantiles, XLF transmitted stress during periods of market stress, most significantly in the latter part of 2020 and early 2021, a period of pandemic-driven uncertainty, fiscal stimulus, and initial signs of inflation. That is an anticipated result from financials — being highly sensitive to credit conditions, interest-rate policy, and general economic health.

Notably, for mid quantiles from late 2020 through mid-2022, XLF's connectedness turns disproportionately negative, signaling a temporary rotation to a shock-absorbing role. It could be evidence of the complacent monetary environment at this time — low rates, healthy capital buffers, and state backstops protecting banks against system stress. For top quantiles, XLF returns to its positive connectedness, and it signals that it supports positive trends. Where economic momentum is high, and rate increases are perceived as good things (proof of growth), financials profit through enhanced margins and credit profile, and they transmit this strength to other markets.

XLB (Materials) is more volatile in its connectedness index but is overall a net transmitter, particularly in the lower and top quantiles. In the 10% quantile, XLB unveils sharp peaks of positive connectedness during late 2020 to early 2021, when supply chain disruptions and early stages of inflationary pressures occurred. In the 30% quantile, XLB is dominated by positive connections, indicating that during benign recessions or early stages of stress, materials dominate in shock transfer, likely due to their exposure to commodity price volatility and changing global demand.

In middle quantiles, XLB's behavior is significantly more irregular. Its role varies with regards to business cycle forecasts and industrial demand. In upper quantiles, XLB reverts to a net transmitter. Stronger commodity prices, increased infrastructure expenditure, and worldwide recovery forces provide materials not only the potential to benefit from rallies but also to pass them on to the rest of the wider market — especially to other cyclicals.

VNQ (Real Estate) shows the most time-varying and quantile-sensitive behavior among the dataset. VNQ is predominantly positive at the 10% quantile, most notably between late 2020 and early 2021, and serves as a transmitter of shocks on the downside. Throughout the low-mid quantiles (20%–70%), VNQ is constantly

negatively correlated with large downward spikes in early 2021 through late 2022 and subsequently from mid-2023 to mid-2024. These periods presumably overlap with Fed rate increases, reduced credit availability, and inflationary pressures that particularly target the property market. VNQ's shock-absorber role aligns with its rate-of-interest responsiveness — it preserves the impact of monetary tightness rather than passing it on to others.

At higher quantiles, VNQ's behavior normalizes — between positive and negative. This suggests that in bull markets, real estate's influence depends on the balance between growth and interest rates. When strong equity performance is coupled with low or stable rates, VNQ may act as a shock transmitter, participating fully in risk-on rallies. Conversely, when rate hikes occur alongside market optimism, VNQ underperforms and reverts to being a receiver due to its rate sensitivity and leveraged nature.

Net Directional Connectedness

At quantile levels from 10% to 30% (tables 14,15,16) the data show that SPY, XLF, and XLB consistently act as strong net transmitters of connectedness, while VIXY tends to be a net receiver with high own variance. It is clear that investors move from risky assets toward safer ones like volatility-related instruments or bonds, causing volatility indices to become more reactive to shocks transmitted from equities and sectors like financials and materials. The relatively low connectedness from VIXY suggests that in less stressed conditions, volatility is less influential on the system.

As market stress increases at quantile levels from 40% to 70% (tables 17,18,19), VIXY's transmission of connectedness rises, and its own variance declines, as volatility becomes more integrated into the system. The increase in total connectedness during these quantiles corresponds to periods of elevated uncertainty and systemic risk. For example, central banks' expansionary policies during the pandemic increased bond market influence, which in turn affected equities and volatility instruments, reinforcing interconnectedness.

At the upper quantile levels from 80% to 90% (tables 20,21), in extreme market stress or crisis states, the data reveal a complex dynamic: VIXY's own variance spikes again, and its net connectedness becomes strongly negative, indicating it is mostly influenced by others rather than transmitting shocks.

SPY remains a prevailing shock transmitter. Several reasons explain why SPY is a leading transmitter. Firstly, its massive market capitalization and liquidity mean that SPY price shocks immediately transmit across financial markets when portfolio managers rebalance portfolios, hedge exposure, or conduct risk rebalancing. This offers a transmission channel for shocks and volatility to pass from SPY to financials like financials (XLF), materials (XLB), real estate (VNQ), and volatility indices (VIXY). Two, SPY embodies broad economic conditions, including corporate earnings, interest

rates, and fiscal policy responses that are crucial to market sentiment during crises. As such macro drivers shift, the SPY price movements function as a measure of systemic risk and are the driver of overall investor sentiment.

4.4 Extreme Value Theory

Upper Quantile

Here, we perform a Generalized Pareto Distribution (GPD) fit to estimate exceedances of financial returns above and below a specified threshold. We are concerned with exceedances above the 95% quantile threshold of return shocks, which captures efficiently the behavior of the extreme upper tail of the distribution. The following table presents the GPD fits for the exceedances above the 95% quantile, including the estimated scale and shape parameters, and their standard errors.

| Fit | Threshold ($u_{U,j}$) | Quantile | Scale Estimate ($\sigma_{j,U}$) | Shape Estimate $\xi_{j,U}$ | Scale (Standard Error) | Shape (Standard Error) |
|-------------------|-------------------------|----------|-----------------------------------|----------------------------|------------------------|------------------------|
| ε_1^N | 1.329182 | 95% | 0.34836251 | 0.02276748 | 0.06017224 | 0.12121213 |
| ε_2^N | 1.956968 | 95% | 0.7230894 | 0.1738579 | 0.1299852 | 0.1327456 |
| ε_3^N | 1.498908 | 95% | 0.4280193 | 0.1491795 | 0.07667172 | 0.13142336 |
| ε_4^N | 1.483115 | 95% | 0.3812620 | 0.2396697 | 0.06894885 | 0.13573447 |
| ε_5^N | 1.521718 | 95% | 0.5154274 | -0.1335011 | 0.09088207 | 0.12731021 |

Table 7: GPD fit to residuals above 95% threshold

Lower Quantile

A similar analysis for the exceedances that fall below the 5% level of returns

| Fit | Threshold ($-u_{D,j}$) | Quantile | Scale Estimate ($\sigma_{D,U}$) | Shape Estimate $\xi_{D,U}$ | Scale SE | Shape SE |
|-------------------|--------------------------|----------|-----------------------------------|----------------------------|------------|------------|
| ε_1^N | 1.874509 | 5% | 0.5791255 | 0.1116706 | 0.1138598 | 0.1539211 |
| ε_2^N | 1.078563 | 5% | 0.3363012 | -0.1911705 | 0.0537642 | 0.1046953 |
| ε_3^N | 1.660046 | 5% | 0.670783937 | 0.001691034 | 0.1351158 | 0.1594444 |
| ε_4^N | 1.690665 | 5% | 0.7461083 | -0.2505941 | 0.1408257 | 0.14638 |
| ε_5^N | 1.695542 | 5% | 0.598470308 | -0.00568697 | 0.09308636 | 0.09508835 |

Table 8: GPD fit to residuals below 5% threshold

Using the GPD estimates of both the upper (above the 95th percentile) and lower (short of the 5th percentile) tails of the standardized residuals, we transformed the standardized data to uniform margins $[0,1]$, through the empirical distribution function (2.5.1). This is a crucial step in copula modeling, whereby it allows us to model the dependence structure and the respective individual marginal distributions independently and separately.

Vine Copula

Second, we employed a Regular Vine (R-Vine) copula, which is especially convenient to apply in multivariate risk management, allowing for high-dimensional copula construction from a cascade of conditioned bivariate copulas on other variables with retained flexibility and interpretability.

| Tree | Pair | Conditioning Set | Copula Family | Parameter 1 | Parameter 2 | Kendall's Tau | UTD | LTD |
|------|----------|------------------|---------------|-------------|-------------|---------------|------|------|
| 1 | SPY-VIXY | - | G90* | -2.35 | 0 | -0.57 | - | - |
| | SPY-VNQ | - | t | 0.68 | 7.24 | 0.48 | 0.25 | 0.25 |
| | XLB-SPY | - | t | 0.76 | 8.77 | 0.55 | 0.28 | 0.28 |
| | XLB-XLF | - | t | 0.77 | 7.75 | 0.56 | 0.32 | 0.32 |
| 2 | XLB-VIXY | SPY | C270* | -0.1 | 0.00 | -0.05 | - | - |
| | XLB-VNQ | SPY | t | 0.28 | 7.50 | 0.18 | 0.06 | 0.06 |
| | XLF-SPY | XLB | t | 0.41 | 7.93 | 0.27 | 0.08 | 0.08 |
| 3 | XLF-VIXY | XLB,SPY | J90* | -1.07 | 0.00 | -0.04 | - | - |
| | XLF-VNQ | XLB,SPY | t | 0.13 | 8.38 | 0.08 | 0.02 | 0.02 |
| 4 | VNQ-VIXY | XLB,SPY | I* | - | - | 0.00 | - | - |

Table 9: R-Vine Copula Dependence Structure

*G90 stands for 90 degree Rotated Gumbel copula, C270 stands for 270 degree Rotated Clayton copula, J90 stands for 90 degree Rotated Joe Copula, t stands for t-Students copula, and I stands for Independence structure.

Goodness of Fit

To evaluate the adequacy of the vine copula model, a Cramér–von Mises (CvM) goodness-of-fit test was conducted. The test produced a CvM statistic of 1.47 and a corresponding p-value of 0.145. As the p-value is greater than the conventional significance level of 0.05, there is insufficient evidence to reject the null hypothesis that the model deviates from the actual distribution. This result suggests that the vine copula model provides an acceptable fit for capturing the dependence structure in the dataset.

The global model fit is quantified additionally by several statistics: log-likelihood = 2405.68, AIC = -4781.35, and BIC = -4703.62. In short, this vine copula model describes a rich and interpretable pattern of dependence among the five financial assets. The strongest and most important dependencies appear in the first tree, namely between SPY–VIXY and SPY–XLB. Conditional dependencies are weakened in higher trees, and most third- and fourth-order interactions are close to conditional independence. The adoption of various copula families, particularly Gumbel and Student-t, is an indication of the necessity to account for both asymmetry and tail dependence.

R-Vine Tree Structure

Figures 52 to 55 depict the Vine copula tree structure through various levels of conditional dependence:

Tree 1: The Primary Dependence Structure (Figure 52)

The first tree models unconditional pairwise dependencies, which serve as the foundation for the general vine structure. The most negative of these is the SPY-VIXY relationship, which is modeled using a 90° degree rotated Gumbel copula (Appendix Bivariate Copulas) with a Kendall's tau of -0.57. Since this type of copula captures lower tail dependencies, a parameter value of -2.35 indicates strong co-movement in economic downturns. This aligns with financial expectation: SPY (a gauge of market performance) and VIXY (a gauge of volatility) tend to move in contrary directions, making them good complements in creating a well-diversified portfolio.

SPY-VNQ pair is positive and moderately strong linear correlation with tau = 0.48 and Student's-t copula par1=0.68. The second parameter of the Student's-t copula indicates moderate upper tail dependence. This indicates that during periods of market stress, SPY maintains a positive association with real estate (VNQ), implying potential resilience or co-movement in the upper tail of the distribution.

Moreover, SPY-XLB ($\tau = 0.55, par1 = 0.76$), and XLF-XLB ($\tau = 0.56, par1 = 0.77$) present moderate to strong upper tail dependence, which characterize sectoral associations that respond similarly to macroeconomic drivers.

Tree 2: Conditional Dependencies Given Key Variables (Figure 53)

Tree 2 examines the dependencies given SPY or XLB, the root nodes of Tree 1. The most significant association is the conditional co-movement relationship between VNQ and XLB with respect to SPY, which suggests a modest positive tau of 0.18 and Student's-t copula parameter 1 of 0.28. This points to a weak tendency for real estate and materials to move together after conditioning for general market index movement and confirms the relationship between financials and the broad market once the material sector movement is controlled for.

Interestingly, the second-order dependence of XLB on VIXY given SPY is described by a C270 copula, has an exceptionally low tau value of -0.05. This indicates a very weak residual dependence between these two variables after conditioning, which means volatility behavior of VIXY and XLB are nearly independent after accounting for market movement.

The edge SPY-XLF conditioned upon XLB represents residual financial dependence on the market overall after adjusting for the impact of the materials sector. Kendall's tau = 0.27 along with Student's-t copula parameter 1 of 0.41, represents moderate positive conditional dependence. SPY and XLF still tend to move similarly after adjustment for the movement of XLB. The low lower and upper tail dependence (0.08 both) indicates that joint extreme movements of SPY and XLF are lower after controlling for XLB. This indicates that XLB explains part but not all of their co-movement, and there remains some independent interaction between SPY and XLF.

Tree 3: Higher-Order, More Complex Dependencies (Figure 54)

Here, the dependency between XLF and VIXY given XLB and SPY is accounted for by a Joe 90 (J90) copula with a near-zero tau of -0.04 and weak lower tail dependence (J90 parameter = -1.07), demonstrating virtually no meaningful dependency. Similarly, XLF and VNQ given XLB and SPY have a very small dependency with tau = 0.08.

These results indicate that all but the most marginal of important dependencies are captured at the first and second levels of the tree. The remaining tail dependence is shown though empirical results to be fairly weak.

Tree 4: Conditional Independence on the Last Level (Figure 55)

In Tree 4, we reach the most primitive level of conditional dependencies. The only edge in this tree, VNQ and VIXY conditioned on SPY, XLF, and XLB, is characterized by

independence. The model asserts there is no remaining residual dependence between VNQ and VIXY after controlling for the remaining assets.

The corresponding Kendall's tau is 0.00, which validates the inference that the pair is conditionally independent under the structure in advance. This last layer guarantees that the existing dependency structure is in Trees 1 and 2 and that higher-order effects are negligible.

Value at Risk

The VaR at the various quantiles for each asset, according to the simulated return distribution, are presented in the table below:

| Quantile | SPY | VIXY | VNQ | XLF | XLB |
|-------------|-------------|-------------|-------------|-------------|-------------|
| 1% (Lower) | -0.04084095 | -0.19108490 | -0.03694728 | -0.04270295 | -0.03836345 |
| 5% (Lower) | -0.01607025 | -0.10528150 | -0.01798615 | -0.02310082 | -0.02020100 |
| 95% (Upper) | 0.03157845 | 0.05571964 | 0.01874674 | 0.01758932 | 0.01652939 |
| 99% (Upper) | 0.05493976 | 0.17193245 | 0.03677312 | 0.03528869 | 0.03394294 |

Table 10: Value at Risk of 1 step ahead forecasted returns

Portfolio Weights

| | w_j^{mvp} | w_j^{mcp} |
|-------------|-------------|-------------|
| SPY | 0.3960 | 0.4377 |
| VIXY | 0.4734 | 0.1959 |
| VNQ | 0.1062 | 0.1223 |
| XLF | 0.0244 | 0.1437 |
| XLB | 0.0000 | 0.1003 |

Table 11: Minimum Variance and Minimum Correlation portfolio weights

Figures 56 to 65 represent the time varying MVP and MCP weights. For the construction of the Value at Risk metric, we will utilize the portfolio weights calculated at time t .

The largest weight values (Table 11) in the minimum variance portfolio are assigned to VIXY (47.3%) and SPY (39.6%), so their combination reduces portfolio volatility while being inversely correlated. Notably, XLB (Materials) is assigned no weight, due to its relatively higher variance or correlation with other assets.

On the other hand, the minimum correlation portfolio allocates weights more evenly on all the assets in the five assets. SPY still has the highest percentage (43.8%), but all assets, such as XLB (10%), are included. This is a statement of a diversification plan to reduce dependence between assets rather than reduce overall volatility.

Portfolio Value at Risk

Value at Risk (VaR) results reveal sharp differences between the minimum variance portfolio and the minimum correlation portfolio in terms of risk-return behavior.

| Percentile | Min Variance VaR | Min Correlation VaR |
|------------|------------------|---------------------|
| 1% | -0.1116 | -0.0698 |
| 5% | -0.0587 | -0.0352 |
| 95% | 0.0413 | 0.0312 |
| 99% | 0.1079 | 0.0707 |

Table 12: Minimum Variance and Minimum Correlation VaR

The minimum variance portfolio is recording prospective losses at extreme quantiles above those of the minimum correlation portfolio, with the former at 1% VaR of -11.16% compared to the latter's -6.98%, indicating greater downside risk in worst-case scenarios. Similarly, its upside gains are more pronounced (e.g., 99% VaR of 10.79% compared with 7.07%), suggesting higher potential for upside but higher volatility. Compared to the minimum correlation portfolio, the former is typically more risk averse, with stricter risk bounds and lower sensitivity to extreme outcomes, both negative and positive.

5. CONCLUSION

This study analyzed the time series behavior of five key financial instruments: SPY (broad equities), VIXY (volatility), XLF (financials), XLB (materials), and VNQ (real estate), over the period from January 1, 2020, to March 31, 2025. To capture the complex dynamics in these markets during turbulent periods, a diverse set of models was applied. These included ARMA with t-students distributed errors, DCC-GARCH models with t-copula dependence structures (using both eGARCH and GJR-GARCH specifications), quantile vector autoregression (QVAR) connectedness, vine copulas, and extreme value theory (EVT).

The ARMA and DCC-GARCH frameworks uncovered distinct patterns of momentum and mean reversion, strong volatility persistence and clustering. The t-copula results confirm moderate tail dependence among the assets and the presence of extreme co-movements. Notably, financial sector (XLF) and volatility (VIXY) exhibit pronounced asymmetric volatility responses to negative shocks, suggesting these sectors amplify downside risks disproportionately.

The total connectedness is highest during extreme market conditions, reflecting increased interdependence during crises such as the COVID-19 pandemic and inflation shocks. The SPY consistently acts as the main transmitter of shocks, shaping overall market dynamics, while VIXY primarily serves as a shock receiver, except during episodes of heightened volatility driven by policy or geopolitical events. Sector-specific indices exhibit varying roles that depend on market regimes and economic conditions.

The vine copula results show that there is a strong inverse relationship between the stock market (SPY) and market volatility (VIXY), meaning when the market goes down, volatility tends to rise sharply. The different sectors within the market, like real estate, materials, and financials, generally move together positively, but not perfectly in sync. When considering the influence of other sectors, these relationships become weaker, indicating that the connections between assets are influenced by multiple factors.

Extreme value theory contributed by quantifying tail risks, showing that SPY and XLF are particularly exposed to downside extremes, while VIXY exhibits sharp upside movements during crises. The Value at Risk (VaR) estimates at multiple quantiles reveal significant tail risks across the ETFs, with VIXY showing the largest potential losses at extreme lower quantiles. Portfolio optimization results show distinct allocation strategies between the minimum variance and minimum correlation portfolios. The minimum variance portfolio concentrates heavily on VIXY (47.3%) and SPY (39.6%). Conversely, the minimum correlation portfolio distributes weights more evenly across assets, including smaller allocations to XLB, aiming to reduce inter-asset dependence rather than volatility alone. Comparing the VaR profiles, the minimum variance portfolio exhibits greater downside risk at the 1% quantile (-11.16%) but also offers higher potential upside (10.79% at 99%), indicating a trade-off between risk and

return due to its concentration in more volatile assets. The minimum correlation portfolio displays lower extreme losses (-6.98%) and gains (7.07%), suggesting a more balanced but less volatile risk profile.

While the combined use of these models offered a robust understanding of return dynamics and interdependence, the analysis is subject to limitations. These include sensitivity to distributional assumptions, potential model misspecification, and the exclusion of regime changes.

In conclusion, this study demonstrates the value of combining traditional time series models with advanced methods for capturing volatility, dependence, and extreme risk in financial markets during periods of upheaval. Such an approach aims to shed light on the behavior of financial markets and is essential for supporting informed decisions in portfolio management and risk oversight.

REFERENCES

- Altinkeski, B. K., Dibooglu, S., Cevik, E. I., Kilic, Y., & Bugan, M. F. (2024).** Quantile connectedness between VIX and global stock markets. *British Journal of Industrial Relations*. <https://doi.org/10.1016/j.bir.2024.07.006>
- Ando, T., Greenwood-Nimmo, M., & Shin, Y. (2018).** Quantile connectedness: Modelling tail behaviour in the topology of financial networks. *SSRN Electronic Journal*. <https://doi.org/10.2139/ssrn.3164772>
- Anscombe, F. J., & Glynn, W. J. (1983).** Distribution of the kurtosis statistic b_2 for normal samples. *Biometrika*, 70(1), 227–234. <https://doi.org/10.1093/biomet/70.1.227>
- Antonakakis, N., Chatziantoniou, I., & Gabauer, D. (2020).** The impact of oil shocks on stock returns: Evidence from regime-switching and Markov-switching GARCH models. *Energy Economics*, 88, 104744. <https://doi.org/10.1016/j.eneco.2020.104744>
- Baur, D. G., & Lucey, B. M. (2010).** Equity market returns in times of crisis. *Journal of Behavioral Finance*, 11(3), 170–182. <https://doi.org/10.1080/15427560.2010.503442>
- Berg, T., & De Smedt, A. (2014).** Modeling financial time series with copulas: A study of systemic risk. *Journal of Financial Econometrics*, 12(1), 1–37. <https://doi.org/10.1093/jjfinec/nbt008>
- Bollerslev, T. (1986).** Generalized Autoregressive Conditional Heteroskedasticity. *Journal of Econometrics*, 31(3), 307–327. [https://doi.org/10.1016/0304-4076\(86\)90063-1](https://doi.org/10.1016/0304-4076(86)90063-1)
- Bollerslev, T. (1990).** Modelling the coherence in short-run nominal exchange rates: A multivariate generalized ARCH model. *The Review of Economics and Statistics*, 72(3), 498–505.
- Box, G. E. P., & Jenkins, G. M. (1970).** *Time series analysis: Forecasting and control*. San Francisco: Holden-Day.
- Christensen, B. J., & Podolskij, M. (2012).** Dynamic copula models and high-frequency data. *Journal of Financial Econometrics*, 10(3), 284–316. <https://doi.org/10.1093/jjfinec/nbt008>
- D’Agostino, R. B. (1970).** Transformation to normality of the null distribution of g_1 . *Biometrika*, 57(3), 679–681. <https://doi.org/10.1093/biomet/57.3.679>
- Diebold, F. X., & Yilmaz, K. (2009).** Measuring financial asset return and volatility spillovers, with application to global equity markets. *The Economic Journal*, 119(534), 158–171. <https://doi.org/10.1111/j.1468-0297.2008.02208.x>

- Diebold, F. X., & Yilmaz, K. (2012).** Better to give than to receive: Predictive directional measurement of volatility spillovers. *International Journal of Forecasting*, 28(1), 57–66. <https://doi.org/10.1016/j.ijforecast.2011.02.006>
- Diebold, F. X., & Yilmaz, K. (2014).** On the network topology of variance decompositions: Measuring the connectedness of financial firms. *Journal of Econometrics*, 182(1), 119–134. <https://doi.org/10.1016/j.jeconom.2014.04.012>
- Elliott, G., Rothenberg, T. J., & Stock, J. H. (1996).** Efficient tests for an autoregressive unit root. *Econometrica*, 64(4), 813–836. <https://doi.org/10.2307/2171846>
- Engle, R. F. (1982).** Autoregressive Conditional Heteroskedasticity with Estimates of the Variance of United Kingdom Inflation. *Econometrica*, 50(4), 987–1007. <https://doi.org/10.2307/1912773>
- Engle, R. F. (2002).** Dynamic conditional correlation: A simple class of multivariate generalized autoregressive conditional heteroskedasticity models. *Journal of Business & Economic Statistics*, 20(3), 339–350.
- Eom, Y. H., Lee, S., & Park, J. (2019).** Measuring tail risk in financial markets. *Journal of Financial Economics*, 133(3), 605–627. <https://doi.org/10.1016/j.jfineco.2019.03.004>
- Financial Times. (2024, May 29).** Low volatility shows investors are underpricing risk. <https://www.ft.com/content/a326d543-6320-44db-bc30-2f6ca8fad824>
- Fisher, L., & Gallagher, L. A. (2012).** New weighted portmanteau statistics for time series goodness-of-fit testing. *Journal of Time Series Analysis*, 33(4), 505–514. <https://doi.org/10.1111/j.1467-9892.2012.00797.x>
- Haluszczynski, A., Laut, I., Modest, H., & R ath, C. (2019).** Linear and nonlinear market correlations: Characterizing financial crises and portfolio optimization. arXiv preprint arXiv:1712.02661. <https://arxiv.org/abs/1712.02661>
- Jajuga, K., Papla, D., & S lepaczuk, R. (2013).** Dynamic linkages between stock markets: The effects of crises and globalization. *Portuguese Economic Journal*, 12(2), 87–112. <https://doi.org/10.1007/s10258-013-0091-1>
- Jarque, C. M., & Bera, A. K. (1980).** Efficient tests for normality, homoscedasticity and serial independence of regression residuals. *Economics Letters*, 6(3), 255–259. [https://doi.org/10.1016/0165-1765\(80\)90024-5](https://doi.org/10.1016/0165-1765(80)90024-5)
- Koliai, L. (2016).** Extreme risk modeling: An EVT–pair-copulas approach for financial stress tests. *Journal of Banking & Finance*, 70, 1–22. <https://doi.org/10.1016/j.jbankfin.2016.02.004>
- Le, T. H., Do, H. X., Nguyen, D. K., & Sensoy, A. (2021).** Covid-19 pandemic and tail-dependency networks of financial assets. *Finance Research Letters*, 38, 101832. <https://doi.org/10.1016/j.frl.2020.101832>

- Liang, C., Hong, Y., Huynh, L.D.T. et al. (2023).** Asymmetric dynamic risk transmission between financial stress and monetary policy uncertainty: thinking in the post-covid-19 world. *Review of Quantitative Finance and Accounting*, 60, 1543–1567. <https://doi.org/10.1007/s11156-023-01140-9>
- Markowitz, H. (1952).** Portfolio selection. *The Journal of Finance*, 7(1), 77–91. <https://doi.org/10.2307/2975974>
- McNeil, A. J., Frey, R., & Embrechts, P. (2005).** *Quantitative Risk Management: Concepts, Techniques, and Tools*. Princeton University Press.
- Nerantzidis, M., Stoupos, N., & Tzeremes, P. (2024).** Realized volatility spillover connectedness among the leading European currencies after the end of the sovereign-debt crisis: A QVAR approach. *Journal of Risk and Financial Management*, 17(8), 337. <https://doi.org/10.3390/jrfm17080337>
- Patton, A. J. (2006).** Modelling asymmetric exchange rate dependence. *International Economic Review*, 47(2), 527–556. <https://doi.org/10.1111/j.1468-0327.2006.00355.x>
- Paul, S., & Sharma, P. (2017).** Improved VaR forecasts using extreme value theory with the Realized GARCH model. *Studies in Economics and Finance*, 34(2), 183–202. <https://doi.org/10.1108/SEF-05-2015-0139>
- Pickands, J. (1975).** Statistical inference using extreme order statistics. *The Annals of Statistics*, 3(1), 119–131. <https://doi.org/10.1214/aos/1176343003>
- Samitas, A., Kenourgios, D., & Paltalidis, N. (2007).** Stock market crashes and expected stock returns: Evidence from the Athens Stock Exchange. *International Review of Financial Analysis*, 16(3), 246–264. <https://doi.org/10.1016/j.irfa.2007.01.005>
- Sklar, A. (1959).** Fonctions de répartition à n dimensions et leurs marges. *Publications de l'Institut de Statistique de l'Université de Paris*, 8, 229–231.
- Sokolinskiy, O. (2020).** Conditional dependence in post-crisis markets: Dispersion and correlation skew trades. *Review of Quantitative Finance and Accounting*, 55(2), 389–426. <https://doi.org/10.1007/s11156-019-00840-5>
- Whittle, P. (1951).** *Hypothesis testing in time series analysis*. Uppsala: Almqvist & Wiksells Boktryckeri AB.
- Xiong, W., & Idzorek, T. (2011).** The investment implications of leverage aversion and financial crises. *Financial Analysts Journal*, 67(5), 29–44. <https://doi.org/10.2469/faj.v67.n5.6>

APPENDIX

Data Plots

Return Plots

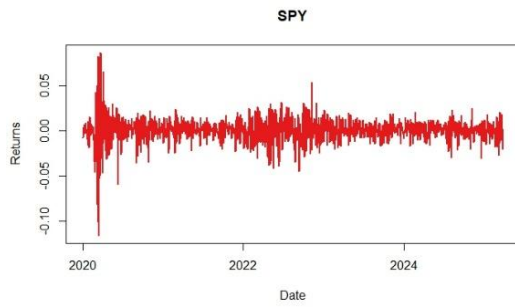


Figure 1: Log Returns of SPY

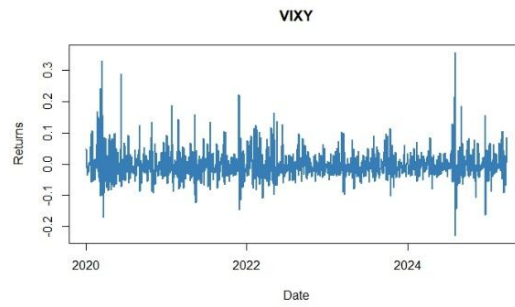


Figure 2: Log Returns of VIXY

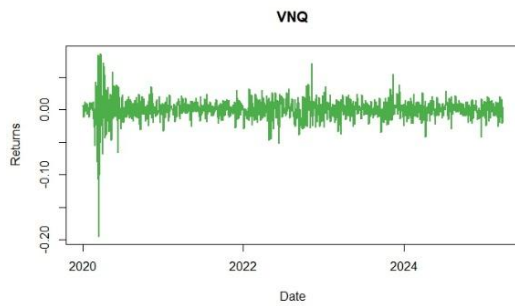


Figure 3: Log Returns of VNQ

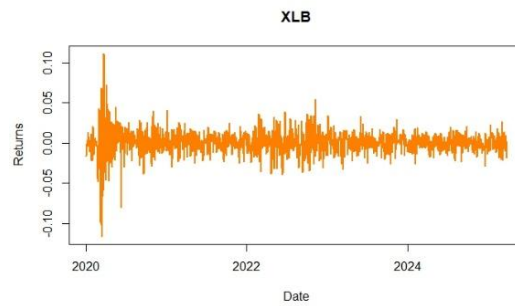


Figure 4: Log Returns of XLB

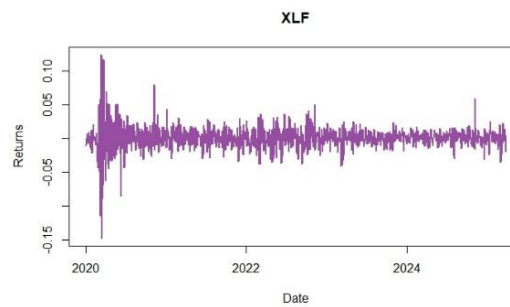


Figure 5: Log Returns of XLF

Summary Statistics

| Statistic | SPY | VIXY | VNQ | XLF | XLB |
|------------------|------------|-------------|------------|------------|------------|
| Min | -0.1158865 | -0.229603 | -0.1951 | -0.1474487 | -0.1166280 |
| 1st Qu. | -0.0052638 | -0.027527 | -0.007122 | -0.0069275 | -0.0072991 |
| Median | 0.0008473 | -0.007699 | 0.0003661 | 0.0007426 | 0.0005868 |
| Mean | 0.0004079 | -0.002235 | -0.0000167 | 0.0003492 | 0.0002563 |
| 3rd Qu. | 0.0072458 | 0.016987 | 0.00772 | 0.0079875 | 0.0082631 |
| Max | 0.0867310 | 0.358031 | 0.08615 | 0.1236025 | 0.1111845 |

Table 13: Summary Statistics for all ETFs

QVAR Connectedness

Total connectedness FROM/TO tables

QUANTILE 10%

| | SPY | VIXY | VNQ | XLF | XLB | FROM |
|---------|------------|-------------|------------|------------|------------|-------------|
| SPY | 27.89 | 6.46 | 21.01 | 22.36 | 22.28 | 72.11 |
| VIXY | 10.30 | 55.34 | 12.41 | 10.88 | 11.07 | 44.66 |
| VNQ | 21.83 | 7.04 | 28.21 | 21.21 | 21.70 | 71.79 |
| XLF | 22.60 | 6.14 | 20.61 | 27.94 | 22.71 | 72.06 |
| XLB | 22.80 | 6.20 | 20.77 | 22.72 | 27.51 | 72.49 |
| TO | 77.53 | 25.84 | 74.80 | 77.17 | 77.76 | 333.11 |
| Inc.Own | 105.43 | 81.18 | 103.01 | 105.11 | 105.27 | cTCI/TCI |
| NET | 5.43 | -18.82 | 3.01 | 5.11 | 5.27 | 83.28/66.62 |
| NPT | 4.00 | 0.00 | 1.00 | 3.00 | 2.00 | |

Table 14: Total Connectedness FROM/TO at 10% level

QUANTILE 20%

| | SPY | VIXY | VNQ | XLF | XLB | FROM |
|---------|------------|-------------|------------|------------|------------|-------------|
| SPY | 32.55 | 2.76 | 19.85 | 22.35 | 22.50 | 67.45 |
| VIXY | 6.20 | 81.84 | 3.69 | 3.98 | 4.29 | 18.16 |
| VNQ | 21.71 | 2.03 | 34.67 | 20.24 | 21.35 | 65.33 |
| XLF | 22.98 | 1.90 | 18.94 | 33.01 | 23.18 | 66.99 |
| XLB | 22.82 | 2.27 | 19.58 | 23.22 | 32.10 | 67.90 |
| TO | 73.71 | 8.96 | 62.07 | 69.79 | 71.32 | 285.83 |
| Inc.Own | 106.26 | 90.79 | 96.73 | 102.80 | 103.42 | cTCI/TCI |
| NET | 6.26 | -9.21 | -3.27 | 2.80 | 3.42 | 71.46/57.17 |
| NPT | 4.00 | 0.00 | 1.00 | 3.00 | 2.00 | |

Table 15: Total Connectedness FROM/TO at 20% level

QUANTILE 30%

| | SPY | VIXY | VNQ | XLF | XLB | FROM |
|---------|--------|--------|-------|--------|--------|-------------|
| SPY | 34.25 | 7.14 | 17.38 | 20.60 | 20.63 | 65.75 |
| VIXY | 14.05 | 66.11 | 5.54 | 7.92 | 6.38 | 33.89 |
| VNQ | 20.18 | 3.66 | 39.05 | 17.90 | 19.20 | 60.95 |
| XLF | 21.44 | 4.58 | 16.44 | 35.55 | 22.00 | 64.45 |
| XLB | 21.65 | 3.64 | 17.29 | 22.24 | 35.18 | 64.82 |
| TO | 77.32 | 19.02 | 56.65 | 68.66 | 68.22 | 289.86 |
| Inc.Own | 111.57 | 85.13 | 95.70 | 104.21 | 103.40 | cTCI/TCI |
| NET | 11.57 | -14.87 | -4.30 | 4.21 | 3.40 | 72.46/57.97 |
| NPT | 4.00 | 0.00 | 1.00 | 3.00 | 2.00 | |

Table 16: Total Connectedness FROM/TO at 30% level

QUANTILE 40%

| | SPY | VIXY | VNQ | XLF | XLB | FROM |
|---------|--------|--------|-------|--------|--------|-------------|
| SPY | 33.34 | 14.65 | 15.25 | 18.45 | 18.31 | 66.66 |
| VIXY | 20.38 | 45.73 | 9.30 | 13.05 | 11.55 | 54.27 |
| VNQ | 18.49 | 8.44 | 40.41 | 15.74 | 16.92 | 59.59 |
| XLF | 19.53 | 10.21 | 14.23 | 35.88 | 20.15 | 64.12 |
| XLB | 20.03 | 9.13 | 15.09 | 20.31 | 35.44 | 64.56 |
| TO | 78.43 | 42.43 | 53.87 | 67.55 | 66.93 | 309.21 |
| Inc.Own | 111.77 | 88.16 | 94.27 | 103.44 | 102.36 | cTCI/TCI |
| NET | 11.77 | -11.84 | -5.73 | 3.44 | 2.36 | 77.30/61.84 |
| NPT | 4.00 | 0.00 | 1.00 | 3.00 | 2.00 | |

Table 17: Total Connectedness FROM/TO at 40% level

QUANTILE 50%

| | SPY | VIXY | VNQ | XLF | XLB | FROM |
|---------|--------|-------|-------|--------|--------|-------------|
| SPY | 32.30 | 18.42 | 14.39 | 17.39 | 17.50 | 67.70 |
| VIXY | 22.13 | 38.28 | 11.08 | 14.85 | 13.65 | 61.72 |
| VNQ | 17.68 | 11.88 | 39.66 | 14.90 | 15.87 | 60.34 |
| XLF | 18.71 | 13.45 | 13.34 | 35.03 | 19.47 | 64.97 |
| XLB | 19.24 | 12.55 | 14.10 | 19.47 | 34.65 | 65.35 |
| TO | 77.76 | 56.30 | 52.91 | 66.61 | 66.50 | 320.08 |
| Inc.Own | 110.06 | 94.58 | 92.58 | 101.63 | 101.15 | cTCI/TCI |
| NET | 10.06 | -5.42 | -7.42 | 1.63 | 1.15 | 80.02/64.02 |
| NPT | 4.00 | 1.00 | 0.00 | 2.00 | 3.00 | |

Table 18: Total Connectedness FROM/TO at 50% level

QUANTILE 60%

| | SPY | VIXY | VNQ | XLF | XLB | FROM |
|---------|--------|-------|-------|--------|--------|-------------|
| SPY | 32.27 | 16.36 | 14.99 | 18.22 | 18.16 | 67.73 |
| VIXY | 21.35 | 41.19 | 10.69 | 13.93 | 12.84 | 58.81 |
| VNQ | 18.25 | 10.36 | 38.70 | 15.79 | 16.90 | 61.30 |
| XLF | 19.47 | 11.55 | 14.23 | 34.55 | 20.21 | 65.45 |
| XLB | 19.79 | 10.69 | 15.06 | 20.14 | 34.32 | 65.68 |
| TO | 78.86 | 48.96 | 54.97 | 68.07 | 68.10 | 318.96 |
| Inc.Own | 111.12 | 90.15 | 93.67 | 102.63 | 102.42 | cTCI/TCI |
| NET | 11.12 | -9.85 | -6.33 | 2.63 | 2.42 | 79.74/63.79 |
| NPT | 4.00 | 0.00 | 1.00 | 2.00 | 3.00 | |

Table 19: Total Connectedness FROM/TO at 60% level

QUANTILE 70%

| | SPY | VIXY | VNQ | XLF | XLB | FROM |
|---------|--------|--------|-------|--------|--------|-------------|
| SPY | 33.10 | 8.53 | 17.46 | 20.41 | 20.51 | 66.90 |
| VIXY | 15.74 | 56.54 | 7.88 | 10.19 | 9.66 | 43.46 |
| VNQ | 20.36 | 5.01 | 37.60 | 17.82 | 19.22 | 62.40 |
| XLF | 21.40 | 6.15 | 16.40 | 34.35 | 21.71 | 65.65 |
| XLB | 21.64 | 5.19 | 17.36 | 21.68 | 34.14 | 65.86 |
| TO | 79.13 | 24.87 | 59.08 | 70.08 | 71.11 | 304.28 |
| Inc.Own | 112.23 | 81.41 | 96.68 | 104.43 | 105.25 | cTCI/TCI |
| NET | 12.23 | -18.59 | -3.32 | 4.43 | 5.25 | 76.07/60.86 |
| NPT | 4.00 | 0.00 | 1.00 | 2.00 | 3.00 | |

Table 20: Total Connectedness FROM/TO at 70% level

QUANTILE 80%

| | SPY | VIXY | VNQ | XLF | XLB | FROM |
|---------|--------|--------|-------|--------|--------|-------------|
| SPY | 32.34 | 2.02 | 20.23 | 22.56 | 22.85 | 67.66 |
| VIXY | 7.93 | 73.29 | 5.84 | 5.92 | 7.02 | 26.71 |
| VNQ | 22.34 | 1.70 | 34.34 | 20.21 | 21.41 | 65.66 |
| XLF | 23.14 | 2.27 | 19.20 | 32.26 | 23.12 | 67.74 |
| XLB | 23.24 | 1.68 | 19.59 | 23.04 | 32.44 | 67.56 |
| TO | 76.65 | 7.68 | 64.85 | 71.74 | 74.40 | 295.32 |
| Inc.Own | 109.00 | 80.97 | 99.19 | 104.00 | 106.84 | cTCI/TCI |
| NET | 9.00 | -19.03 | -0.81 | 4.00 | 6.84 | 73.83/59.06 |
| NPT | 4.00 | 0.00 | 1.00 | 2.00 | 3.00 | |

Table 21: Total Connectedness FROM/TO at 80% level

QUANTILE 90%

| | SPY | VIXY | VNQ | XLF | XLB | FROM |
|---------|------------|-------------|------------|------------|------------|-------------|
| SPY | 27.90 | 6.48 | 20.91 | 22.14 | 22.57 | 72.10 |
| VIXY | 12.58 | 46.55 | 14.30 | 12.88 | 13.70 | 53.45 |
| VNQ | 21.51 | 8.38 | 28.19 | 20.57 | 21.35 | 71.81 |
| XLF | 22.61 | 6.79 | 20.19 | 27.86 | 22.55 | 72.14 |
| XLB | 22.57 | 6.45 | 20.51 | 22.48 | 27.98 | 72.02 |
| TO | 79.26 | 28.10 | 75.90 | 78.08 | 80.17 | 341.51 |
| Inc.Own | 107.16 | 74.65 | 104.09 | 105.94 | 108.15 | cTCI/TCI |
| NET | 7.16 | -25.35 | 4.09 | 5.94 | 8.15 | 85.38/68.30 |
| NPT | 4.00 | 0.00 | 1.00 | 2.00 | 3.00 | |

Table 22: Total Connectedness FROM/TO at 90% level

QVAR Directional Connectedness (FROM)

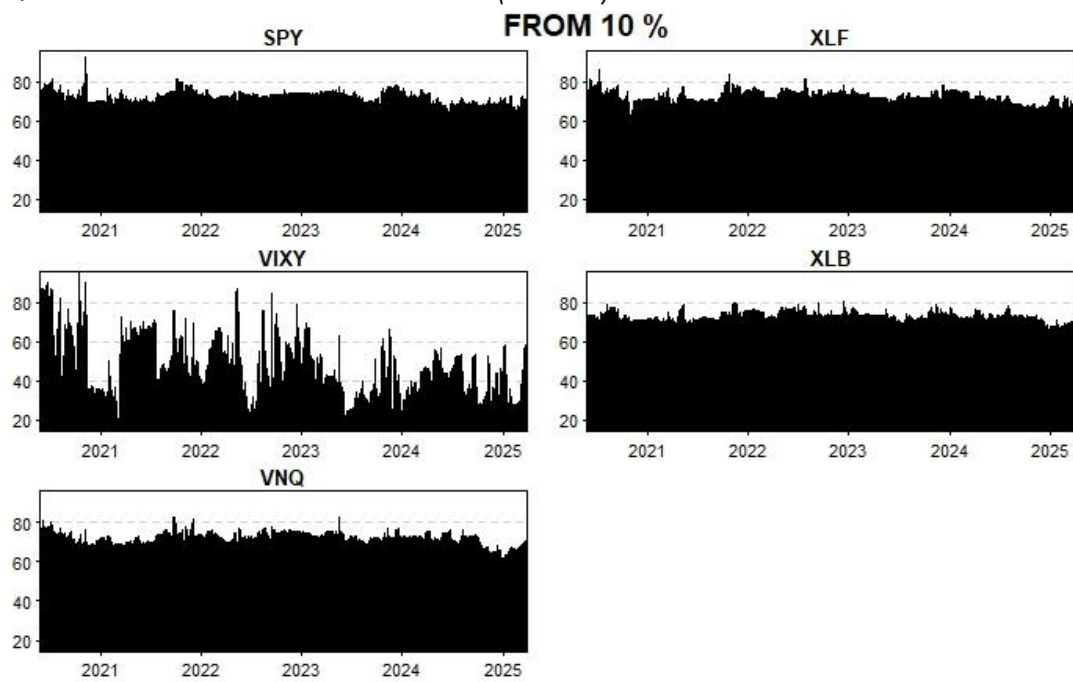


Figure 6: QVAR Directional Connectedness (FROM) at level 10%

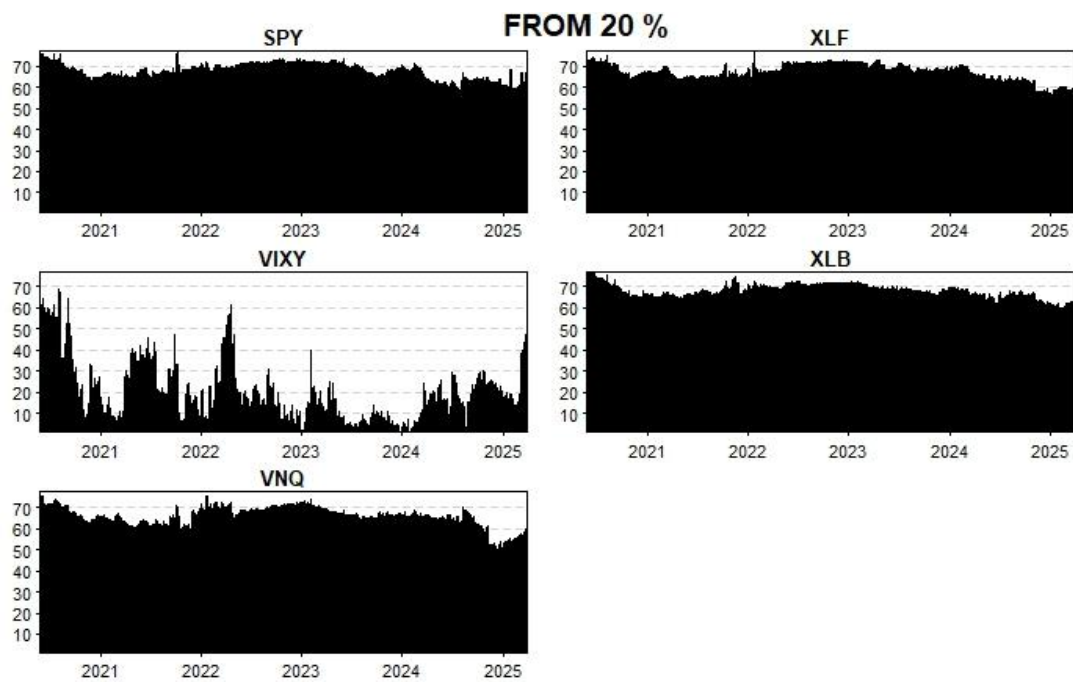


Figure 7: QVAR Directional Connectedness (FROM) at level 20%

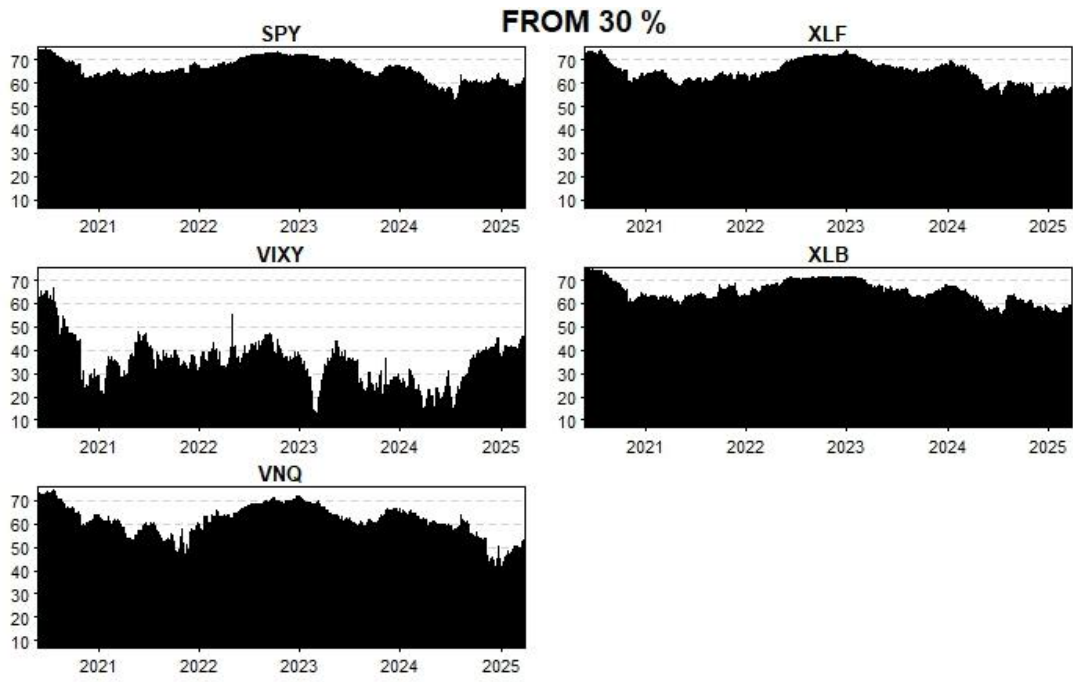


Figure 8: QVAR Directional Connectedness (FROM) at level 30%

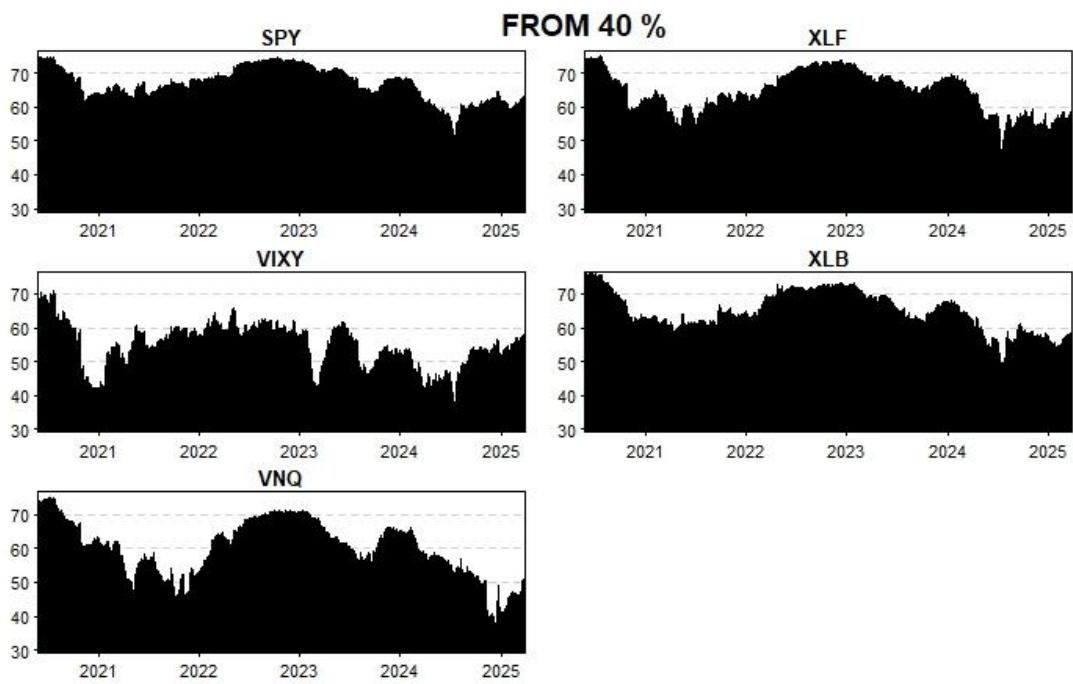


Figure 9: QVAR Directional Connectedness (FROM) at level 40%

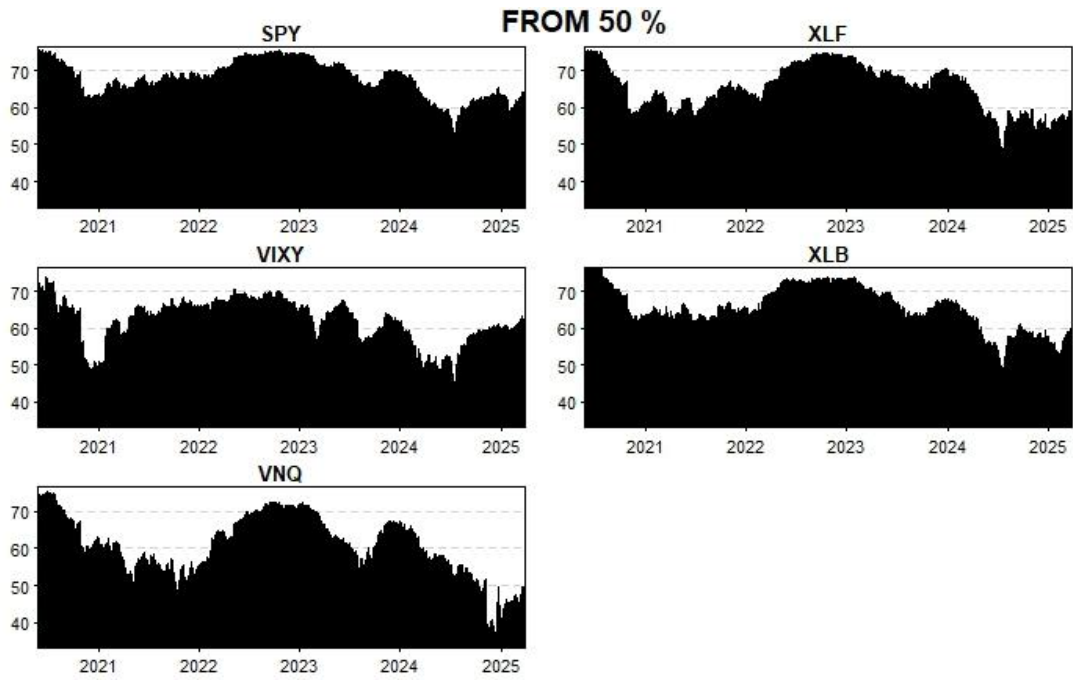


Figure 10: QVAR Directional Connectedness (FROM) at level 50%

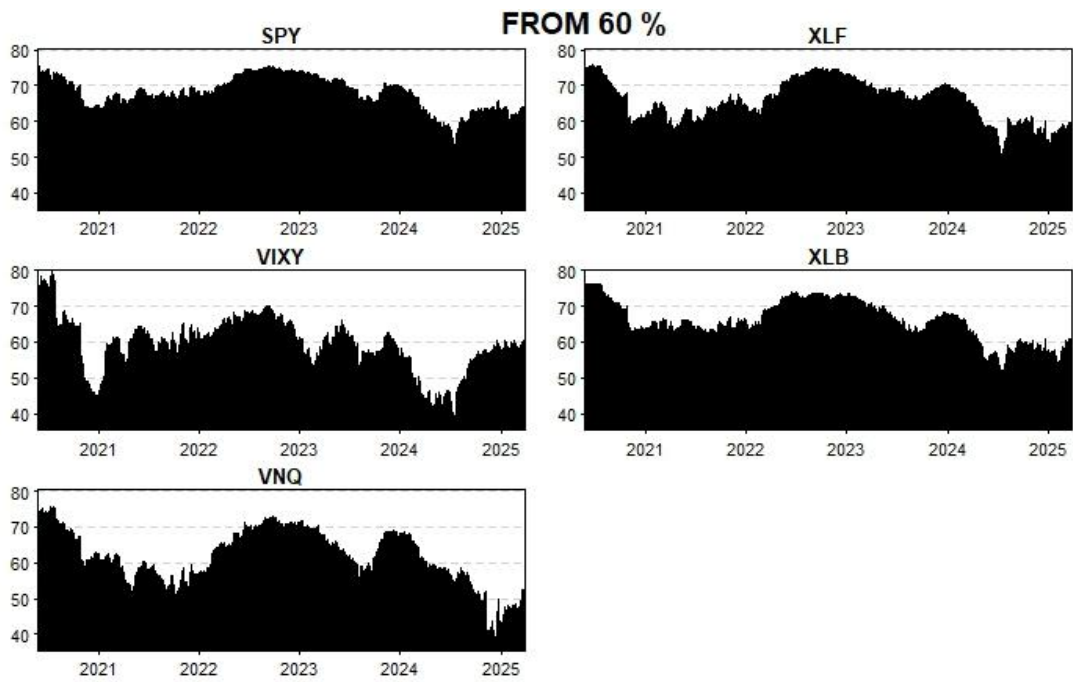


Figure 11: QVAR Directional Connectedness (FROM) at level 60%

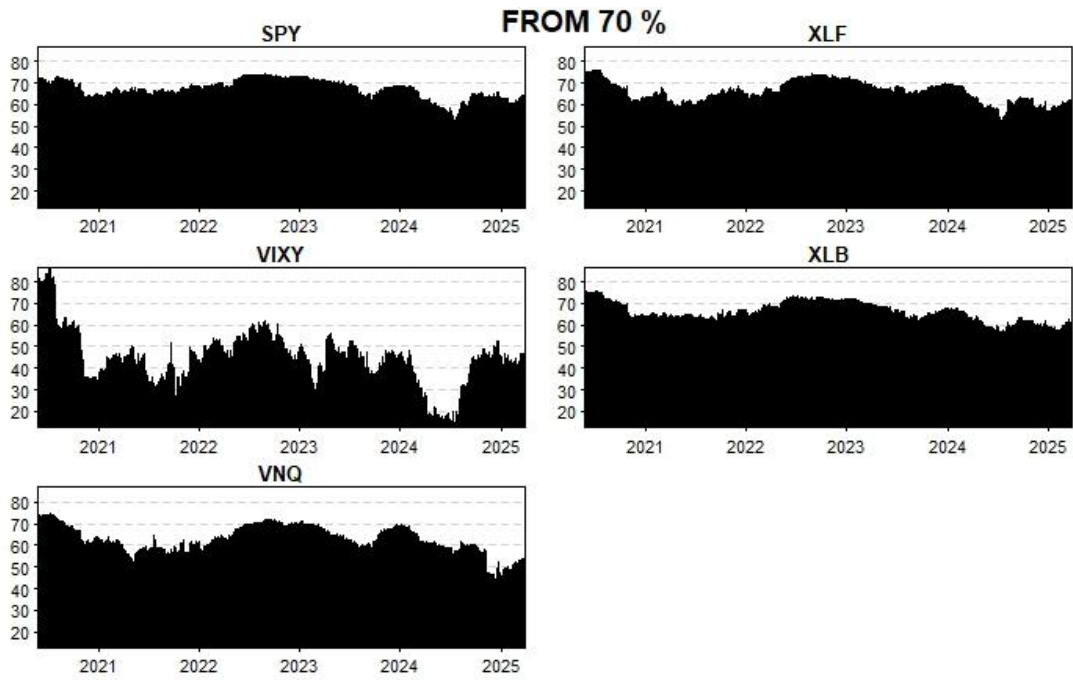


Figure 12: QVAR Directional Connectedness (FROM) at level 70%

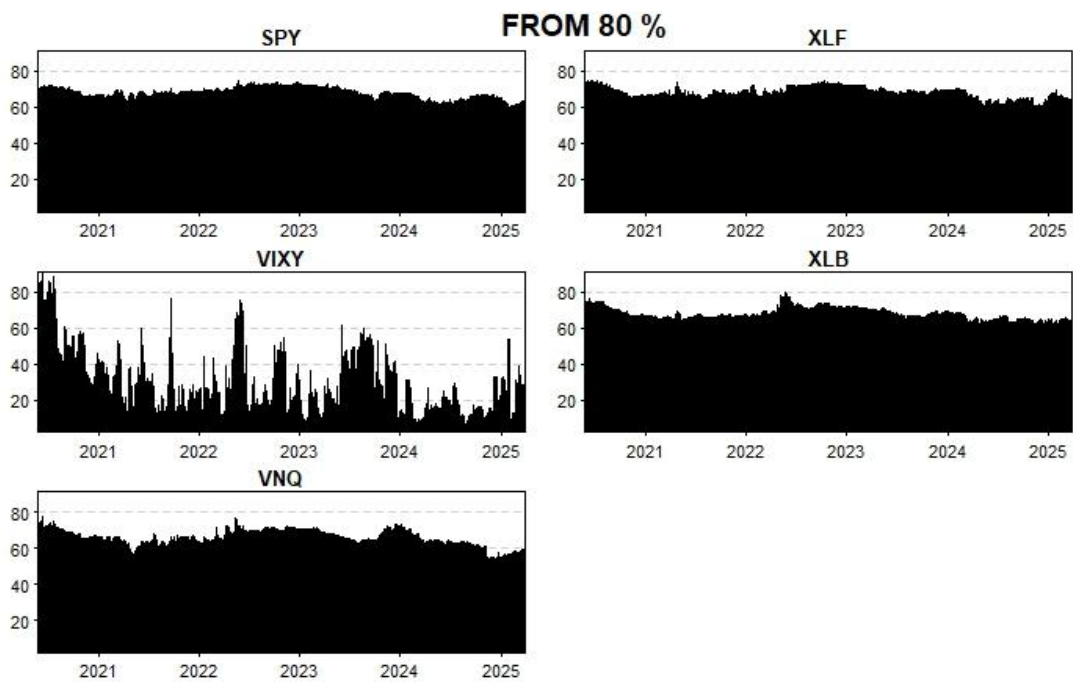


Figure 13: QVAR Directional Connectedness (FROM) at level 80%

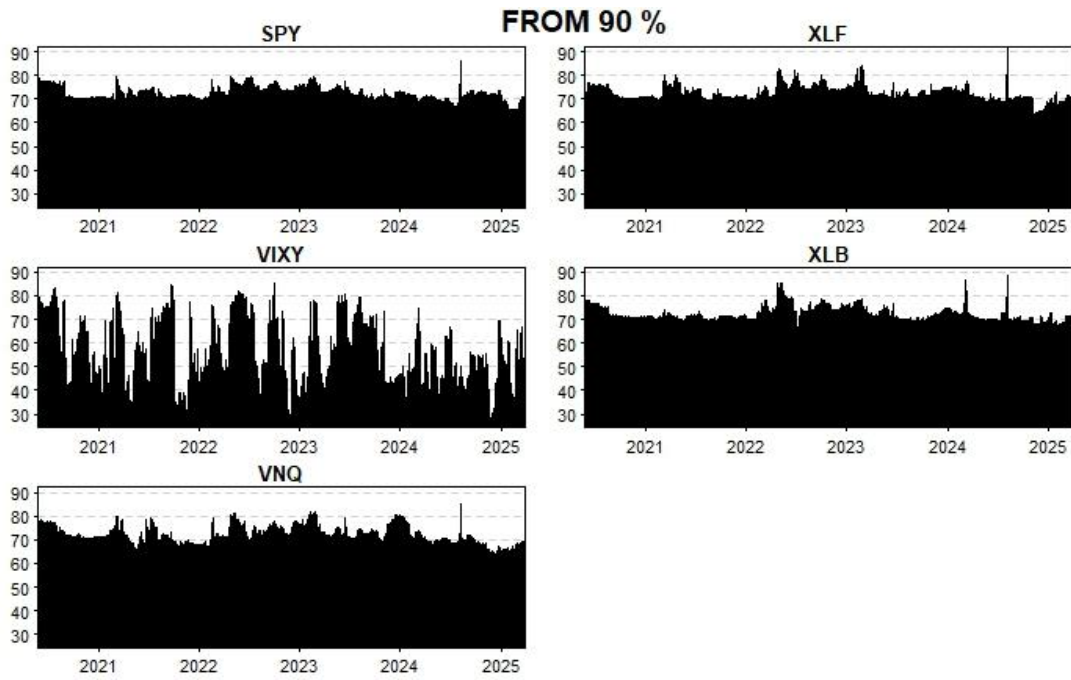


Figure 14: QVAR Directional Connectedness (FROM) at level 90%

QVAR Directional Connectedness (TO)

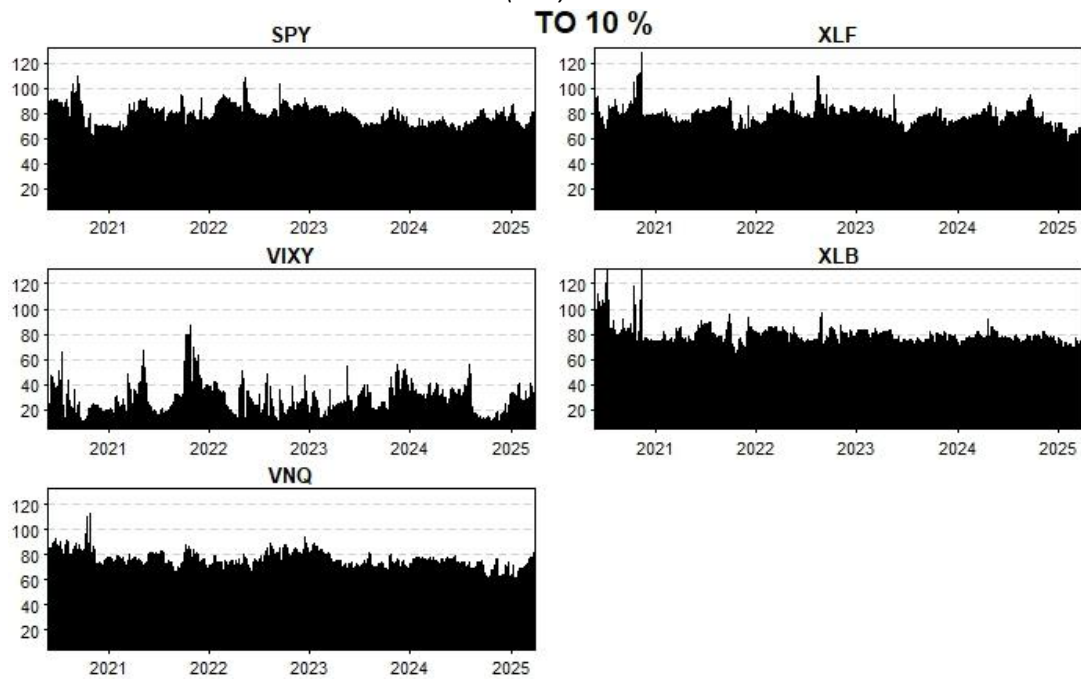


Figure 15: QVAR Directional Connectedness (TO) at level 10%

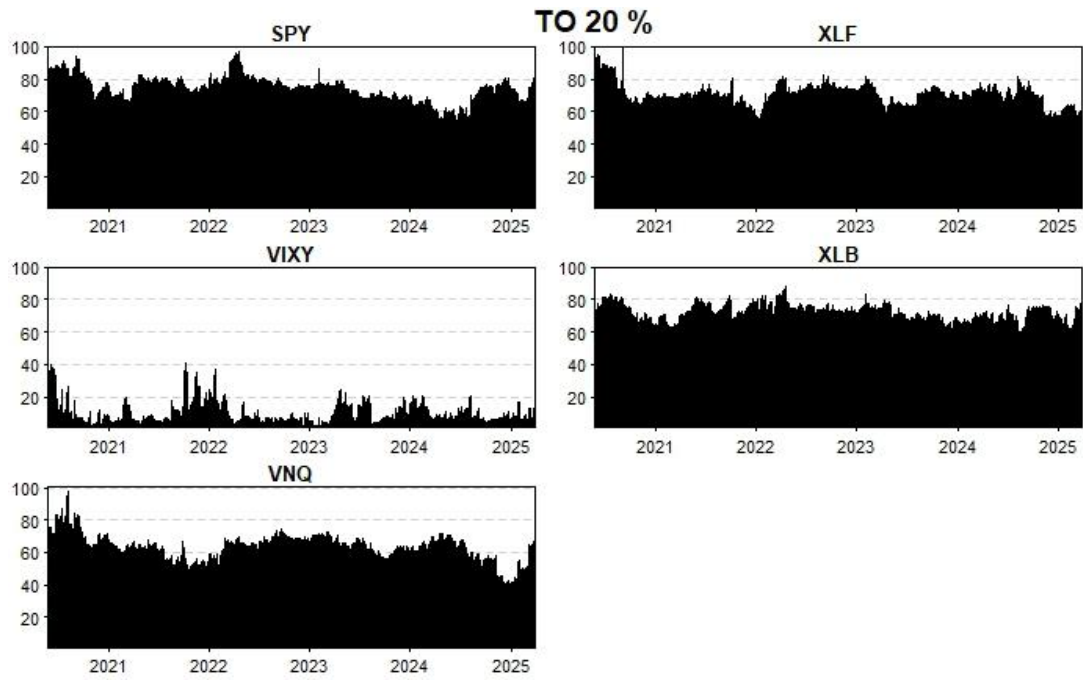


Figure 16: QVAR Directional Connectedness (TO) at level 20%

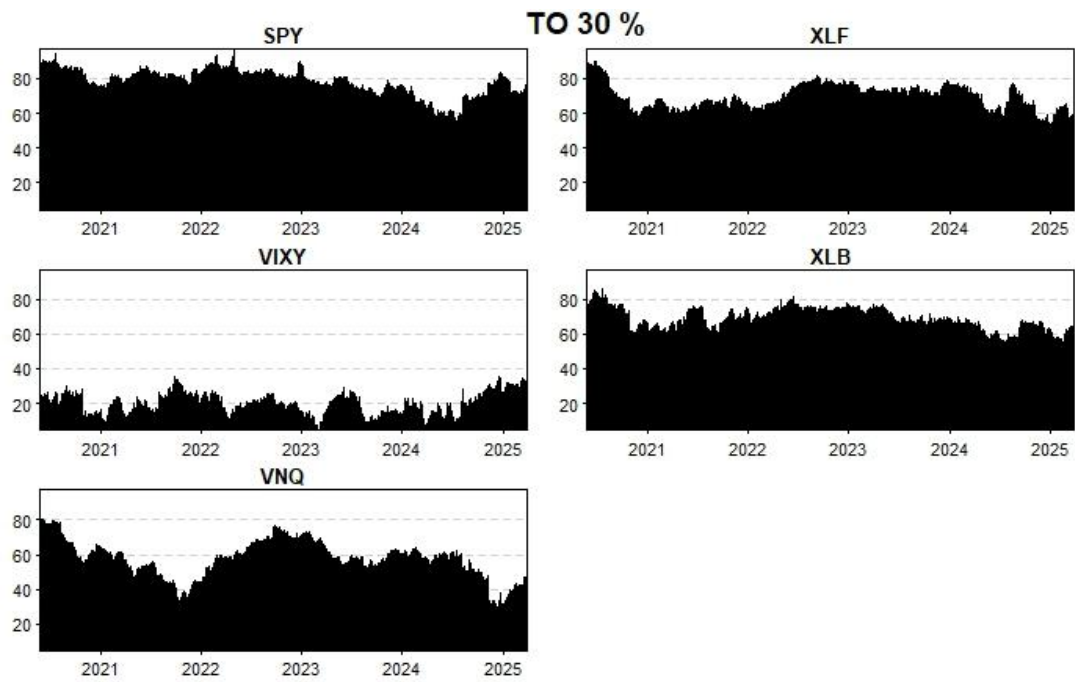


Figure 17: QVAR Directional Connectedness (TO) at level 30%

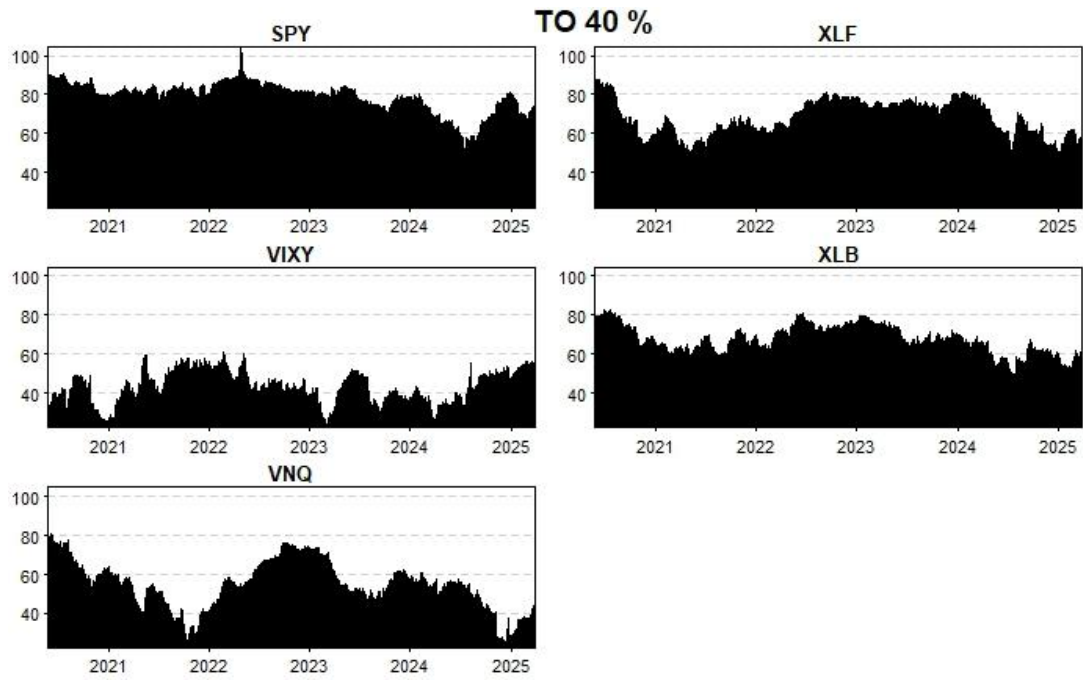


Figure 18: QVAR Directional Connectedness (TO) at level 40%

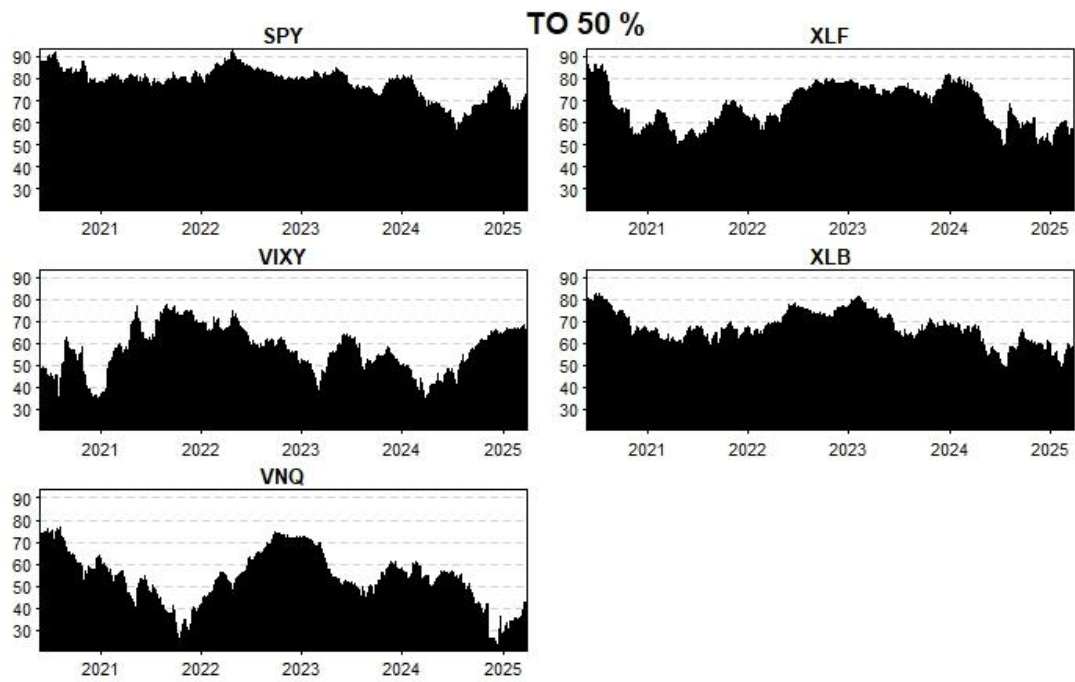


Figure 19: QVAR Directional Connectedness (TO) at level 50%

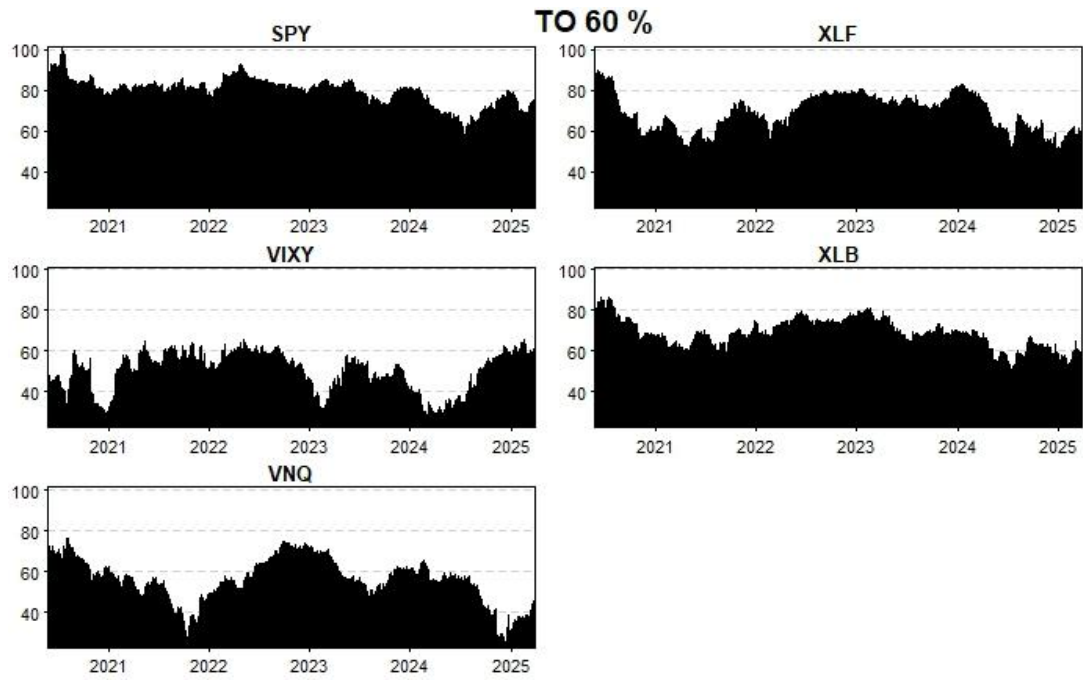


Figure 20: QVAR Directional Connectedness (TO) at level 60%

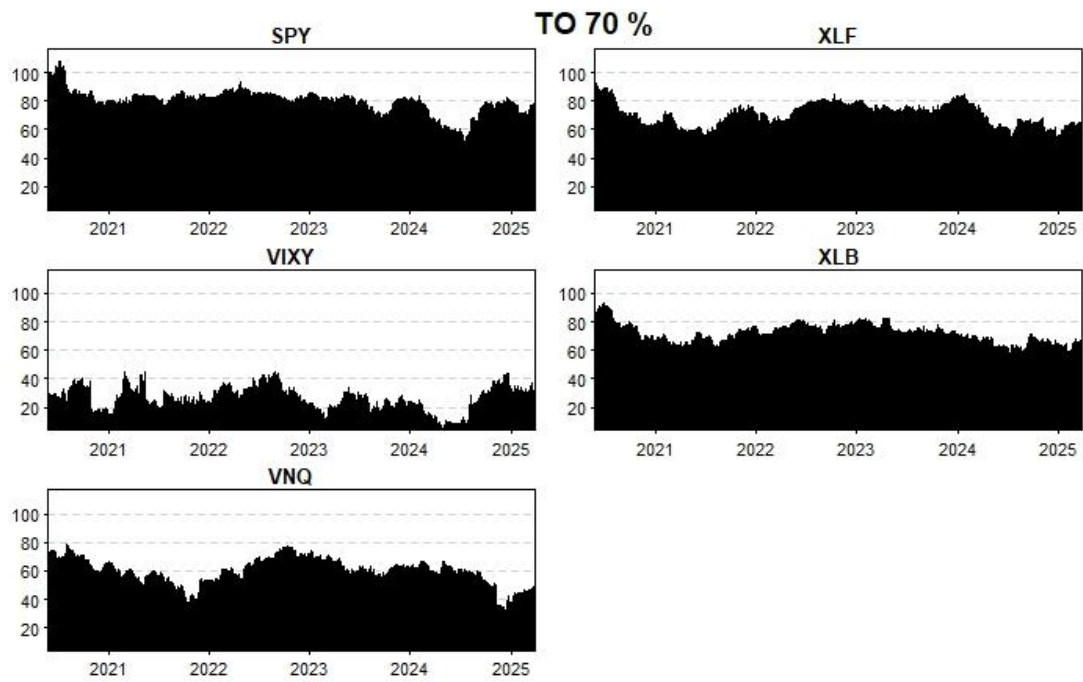


Figure 21: QVAR Directional Connectedness (TO) at level 70%

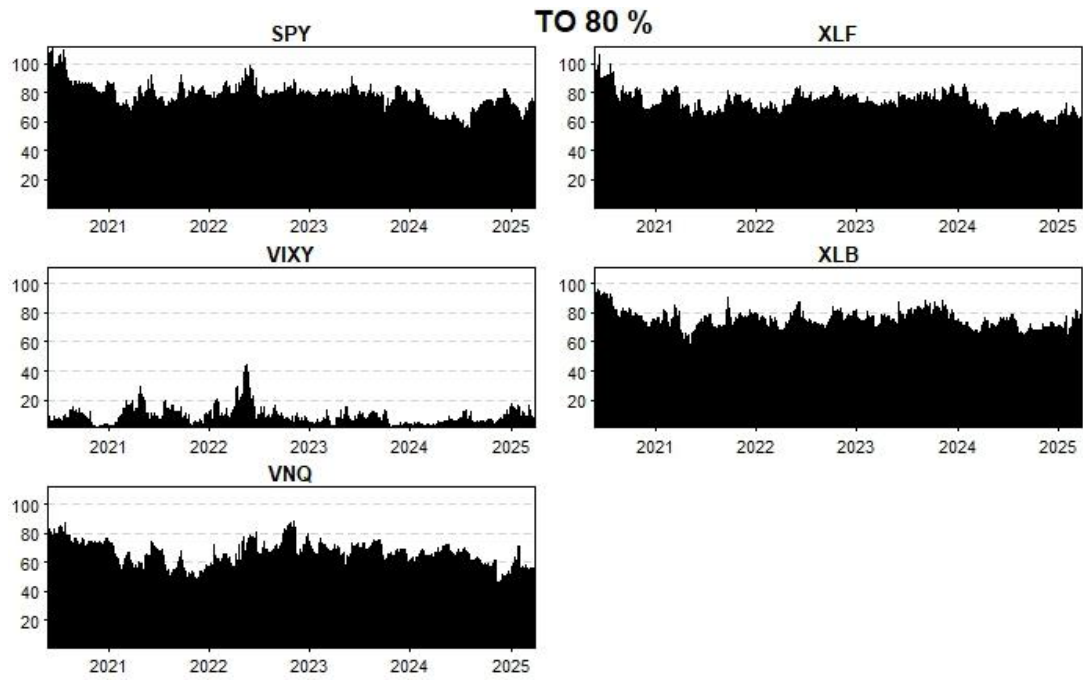


Figure 22: QVAR Directional Connectedness (TO) at level 80%

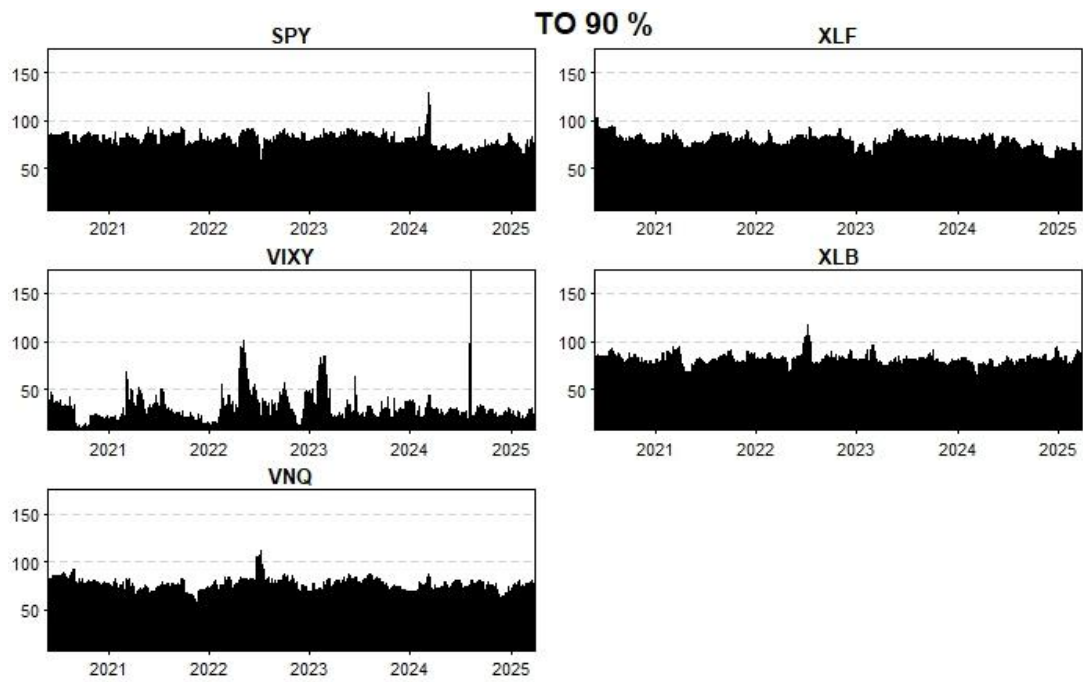


Figure 23: QVAR Directional Connectedness (TO) at level 80%

QVAR Total Connectedness Index Plot

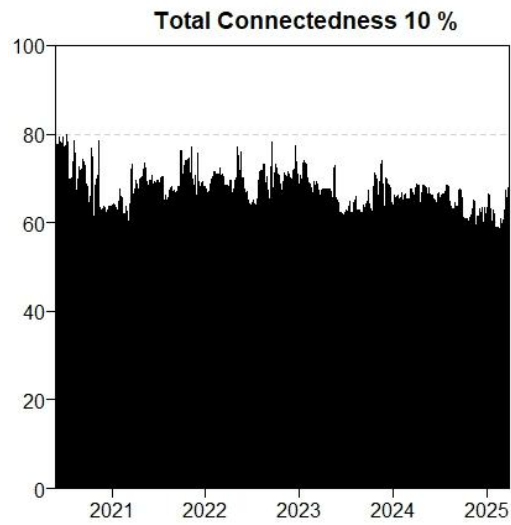


Figure 24: QVAR Total Connectedness 10%

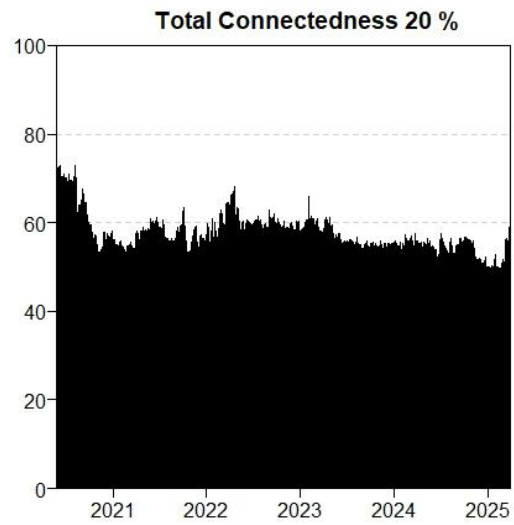


Figure 25: QVAR Total Connectedness 20%

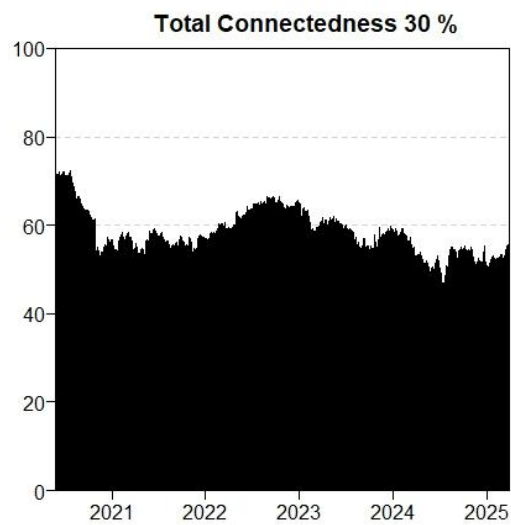


Figure 26: QVAR Total Connectedness 30%

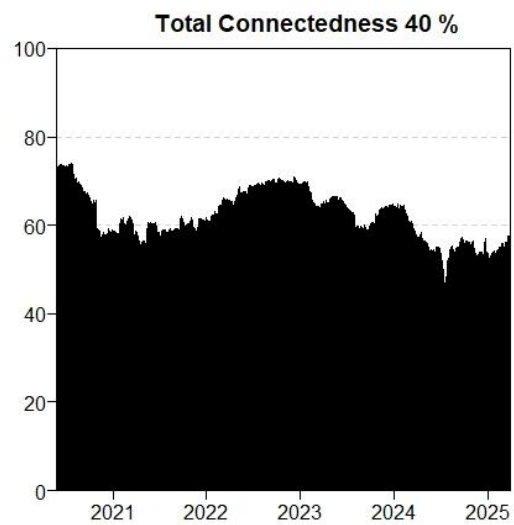


Figure 27: QVAR Total Connectedness 40%

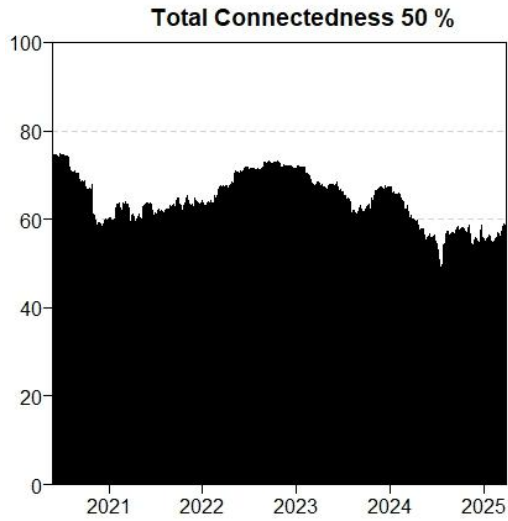


Figure 28: QVAR Total Connectedness 50%

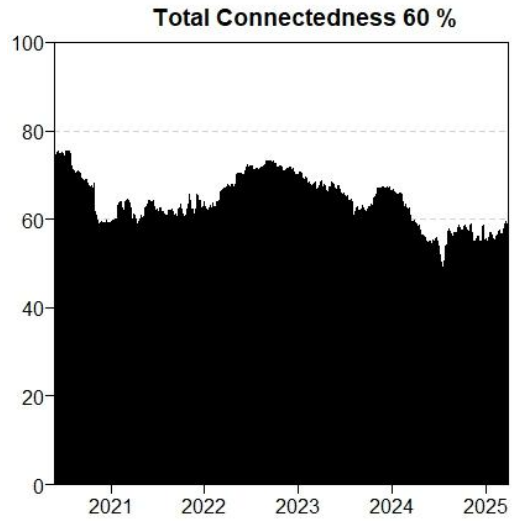


Figure 29: QVAR Total Connectedness 60%

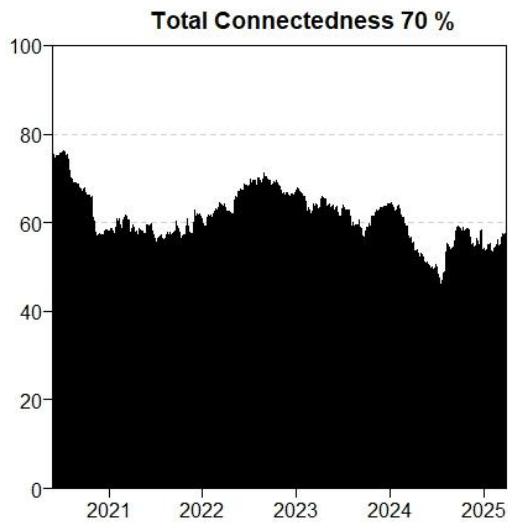


Figure 30: QVAR Total Connectedness 70%

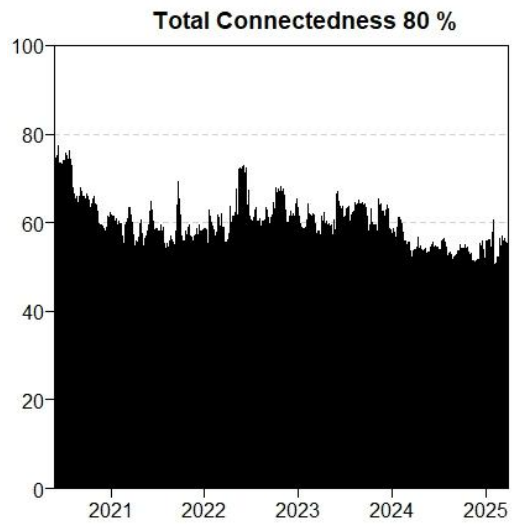


Figure 31: QVAR Total Connectedness 80%

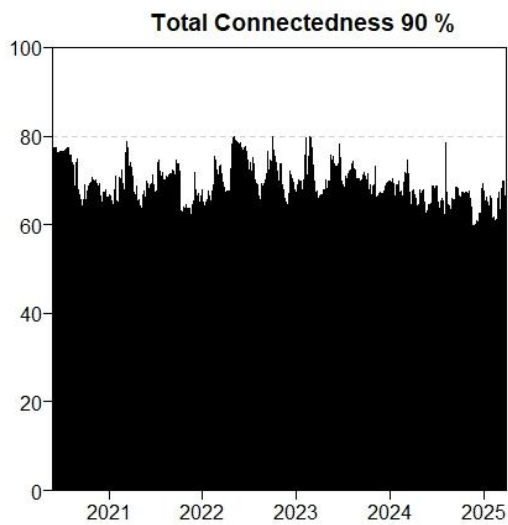


Figure 32: QVAR Total Connectedness 90%

QVAR Net Connectedness Plot

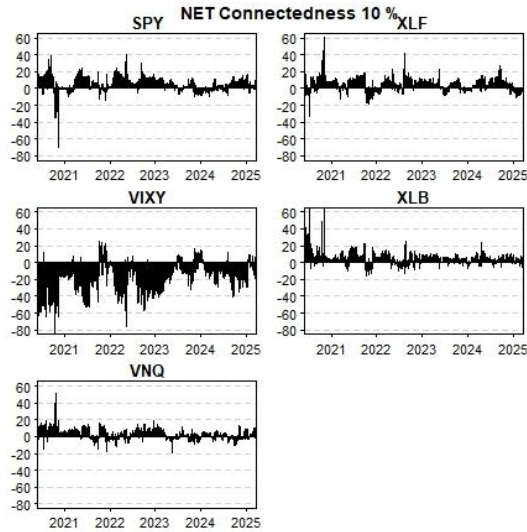


Figure 33: QVAR NET Connectedness 10%

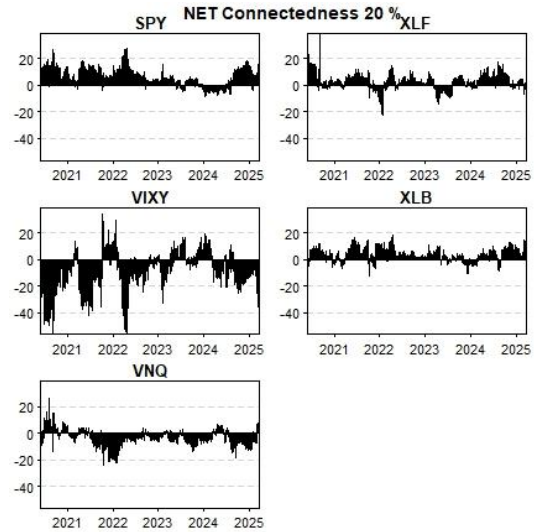


Figure 34: QVAR NET Connectedness 20%

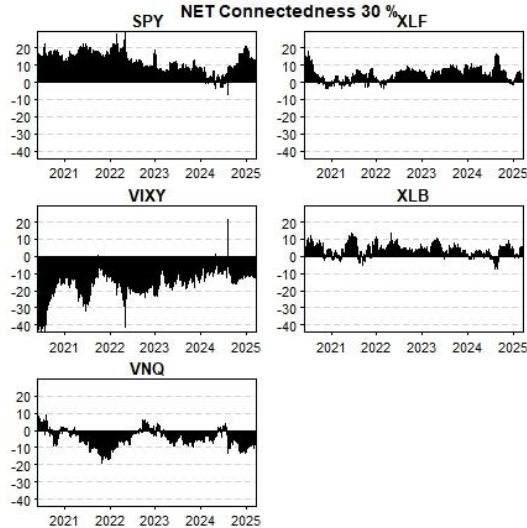


Figure 35: QVAR NET Connectedness 30%

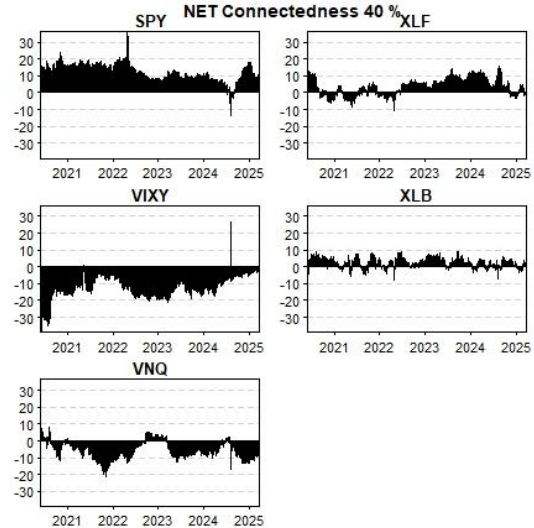


Figure 36: QVAR NET Connectedness 40%

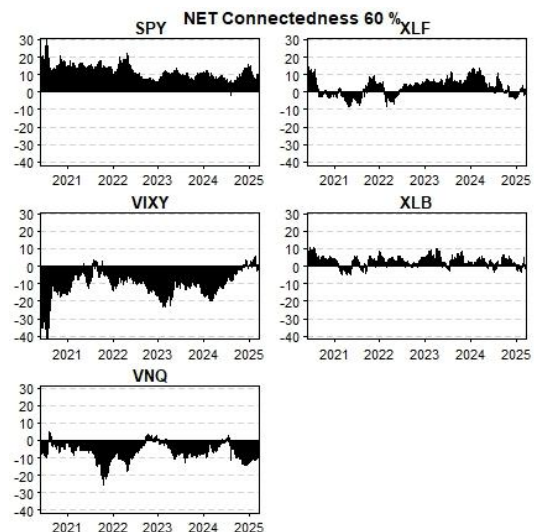
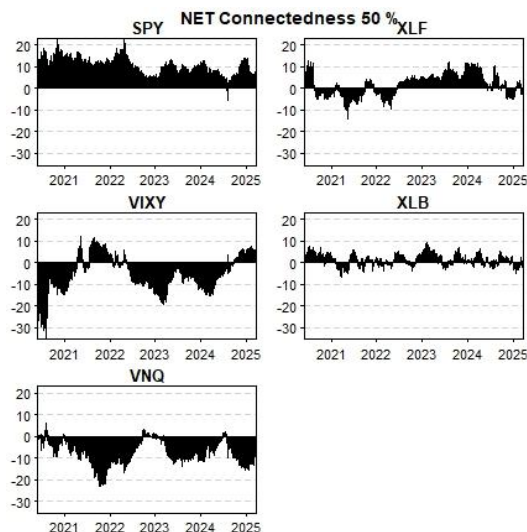


Figure 37: QVAR NET Connectedness 50%

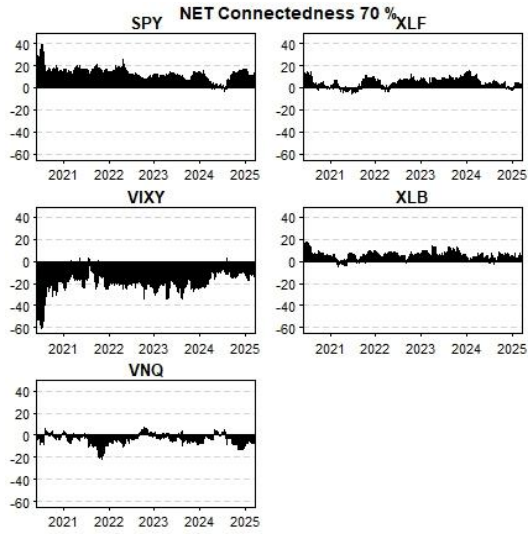


Figure 38: QVAR NET Connectedness 60%

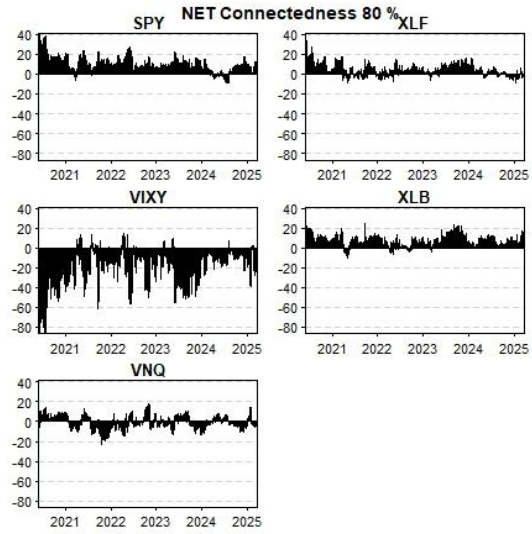


Figure 39: QVAR NET Connectedness 70%

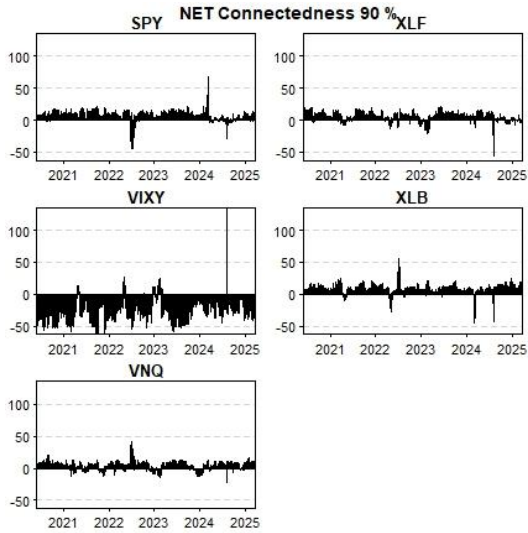
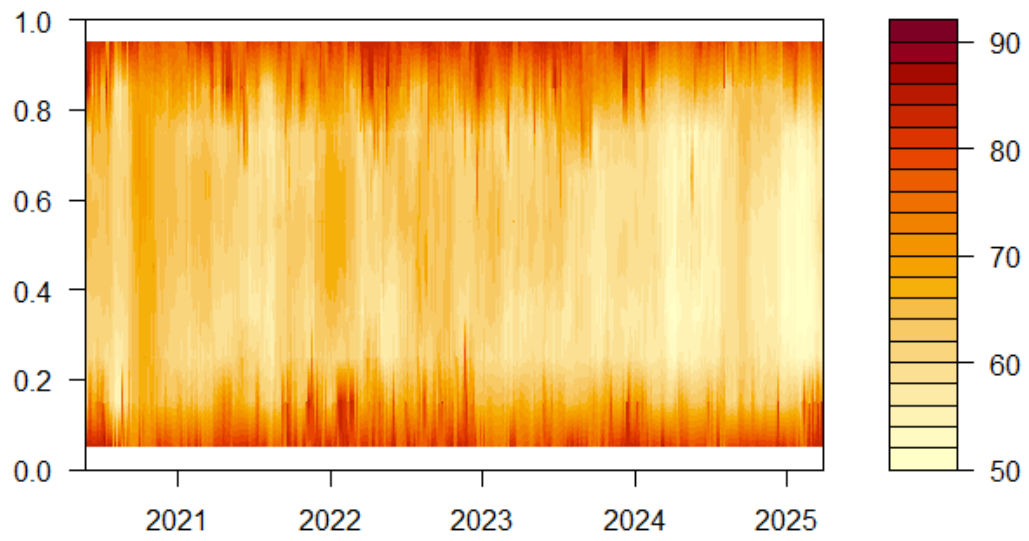


Figure 40: QVAR NET Connectedness 80%



Figure 41: QVAR NET Connectedness 90%



QVAR Connectedness Heatmap Plot**Figure 42:** QVAR Heatmap

QVAR Network Plot

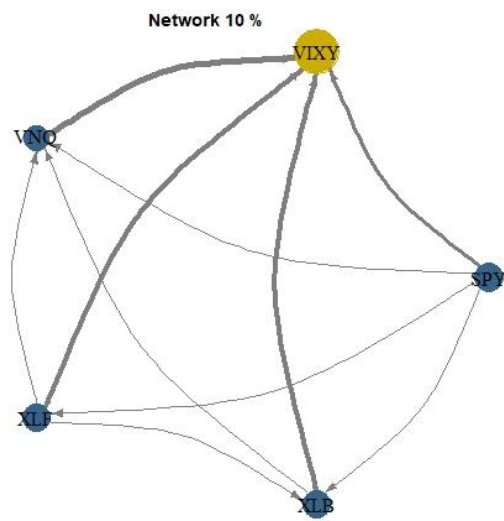


Figure 43: QVAR NETWORK PLOT 10%

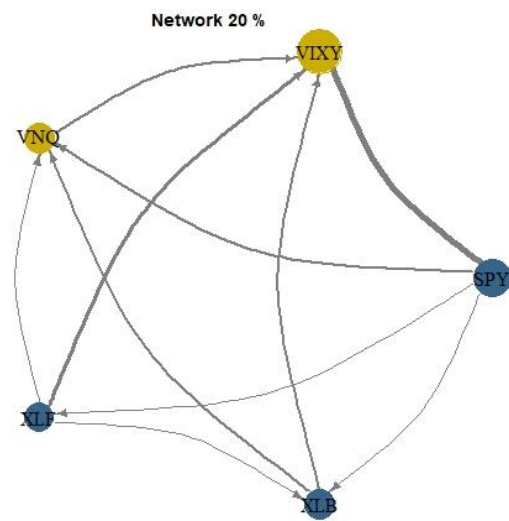


Figure 44: QVAR NETWORK PLOT 20%

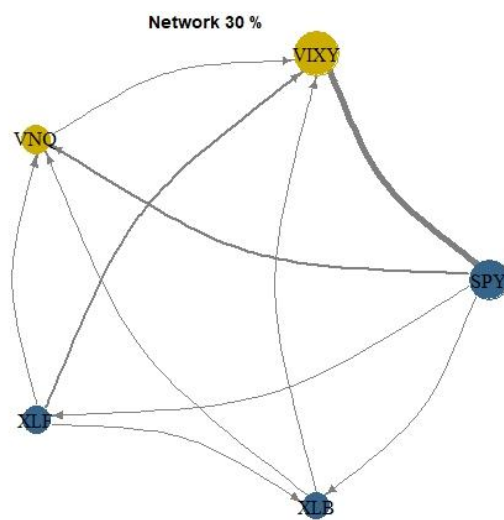


Figure 45: QVAR NETWORK PLOT 30%

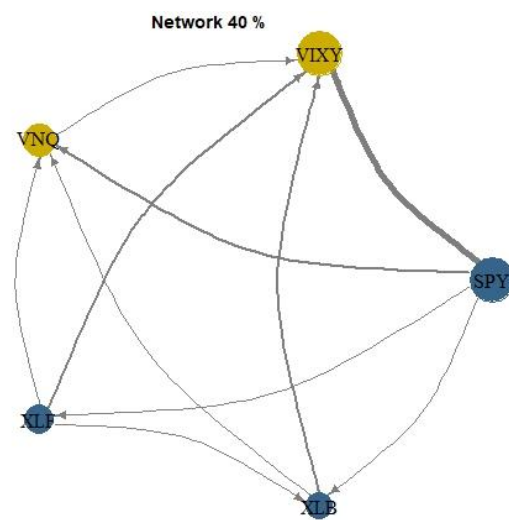


Figure 46: QVAR NETWORK PLOT 40%

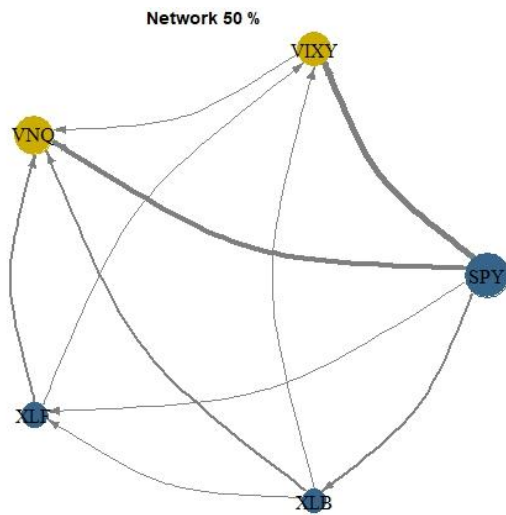


Figure 47: QVAR NETWORK PLOT 50%

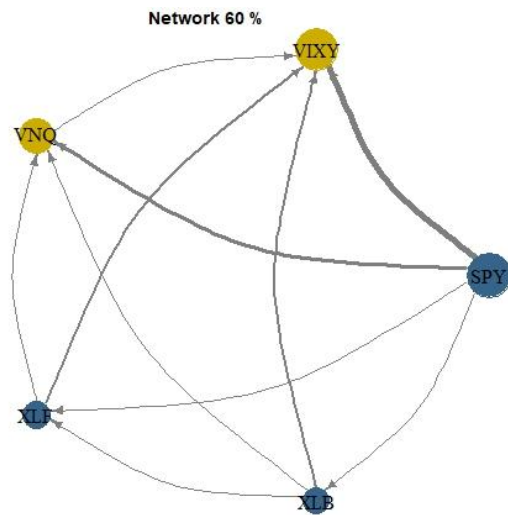


Figure 48: QVAR NETWORK PLOT 60%

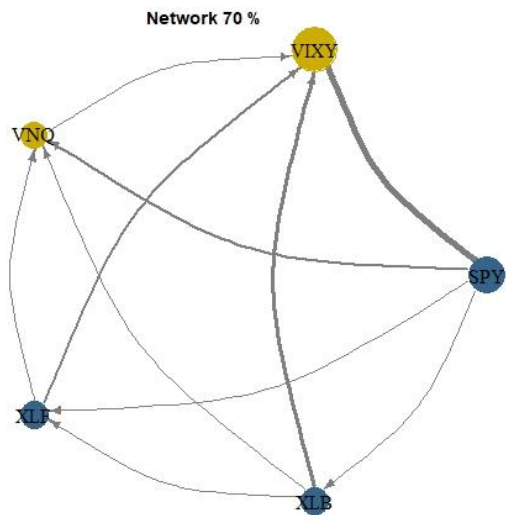


Figure 49: QVAR NETWORK PLOT 70%

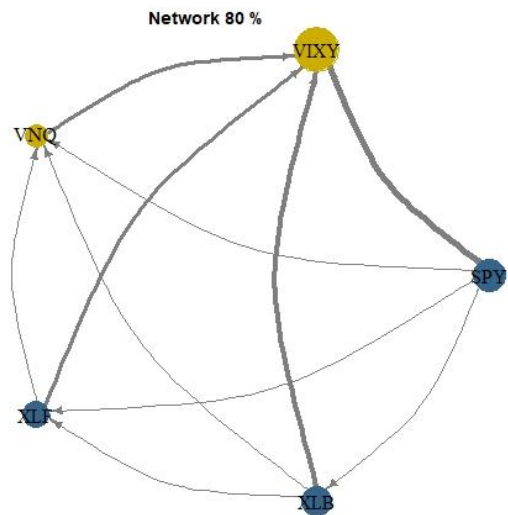


Figure 50: QVAR NETWORK PLOT 80%

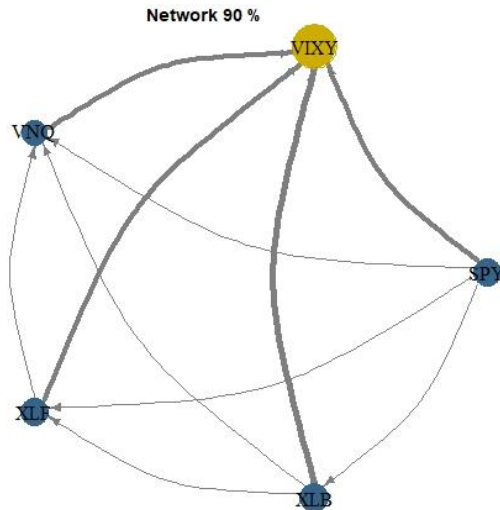


Figure 51: QVAR NETWORK PLOT 90%

Extreme Value Theory

Summary Statistics of empirical returns

| Statistic | SPY | VIXY | VNQ | XLF | XLB |
|------------------|------------|-------------|------------|------------|------------|
| Min. | -0.371553 | -1.047215 | -0.158078 | -0.108937 | -0.127818 |
| 1st Qu. | 0.002905 | -0.042637 | -0.003675 | -0.007055 | -0.006219 |
| Median | 0.007768 | -0.024830 | 0.000289 | -0.002562 | -0.002046 |
| Mean | 0.007718 | -0.023944 | 0.000355 | -0.002570 | -0.002114 |
| 3rd Qu. | 0.012766 | -0.007318 | 0.004393 | 0.001868 | 0.001946 |
| Max. | 0.339047 | 1.324030 | 0.268601 | 0.204992 | 0.183219 |

Table 23: Summary Statistics for 1 step ahead empirical return prediction

Summary Statistics of empirical residuals

| Statistic | SPY | VIXY | VNQ | XLF | XLB |
|------------------|------------|-------------|------------|------------|------------|
| Min. | -9.18157 | -2.33450 | -5.24103 | -4.01878 | -6.17475 |
| 1st Qu. | -0.75511 | -0.44300 | -0.66999 | -0.69629 | -0.67918 |
| Median | -0.06339 | 0.14740 | -0.00882 | -0.01724 | -0.01930 |
| Mean | -0.13717 | 0.25300 | -0.03477 | -0.05344 | -0.04129 |
| 3rd Qu. | 0.55823 | 0.79970 | 0.63313 | 0.63491 | 0.62880 |
| Max. | 3.81132 | 17.61380 | 6.37212 | 7.13876 | 3.50619 |

Table 24: Summary Statistics for 1 step ahead empirical residuals prediction

R-Vine Bivariate Copulas

90-degree Rotated Gumbel Copula

$$C_{G90}(u_1, u_2) = u_2 - \exp \left\{ - \left[(-\ln(u_1))^{\vartheta_G} + (-\ln(1 - u_2))^{\vartheta_G} \right]^{\frac{1}{\vartheta_G}} \right\}$$

Where ϑ_G denotes the Gumbel Copula dependence parameter

270-degree Rotated Clayton Copula

$$C_{C270, \vartheta_C}(u_1, u_2) = u_1 - \left[u_1^{-\vartheta_C} + (1 - u_2)^{-\vartheta_C} - 1 \right]^{\frac{1}{\vartheta_C}}$$

Where ϑ_C denotes the Clayton Copula dependence parameter

90-degree Rotated Joe Copula

$$C_{J90, \vartheta_J}(u_1, u_2) = u_1 - 1 + \left[u_1^{\vartheta_J} + (1 - u_2)^{\vartheta_J} - u_1^{\vartheta_J} (1 - u_2)^{\vartheta_J} \right]^{\frac{1}{\vartheta_J}}$$

Where ϑ_J denotes the Joe Copula dependence parameter

R-Vine Structure Plots

Tree 1

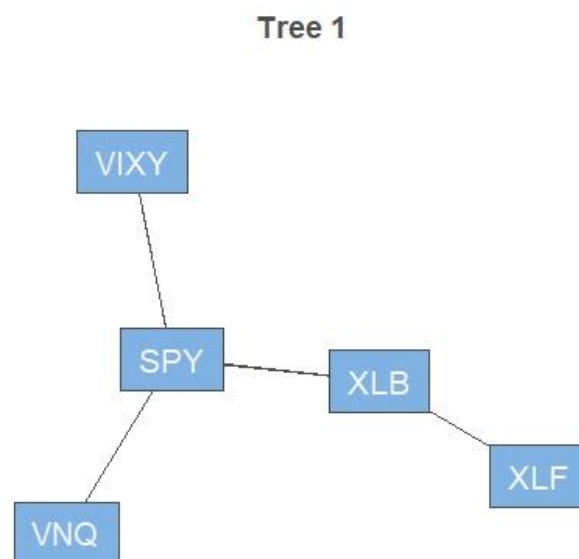


Figure 52: R-Vine Copula Conditional Dependence Tree (1)

Tree 2

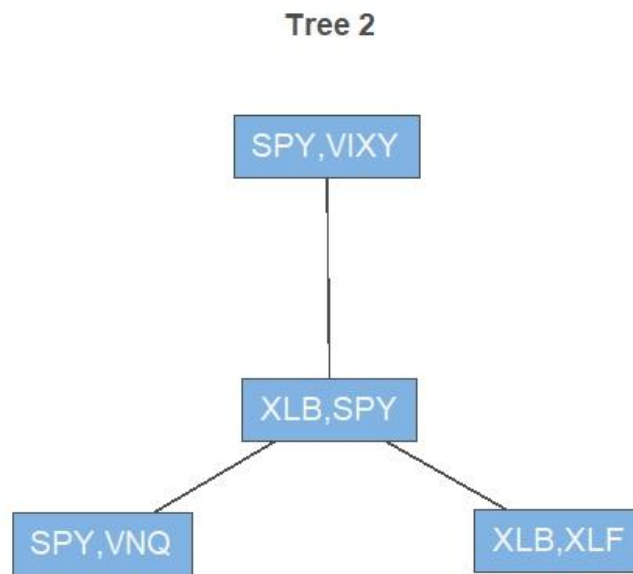


Figure 53: R-Vine Copula Conditional Dependence Tree (2)

Tree 3

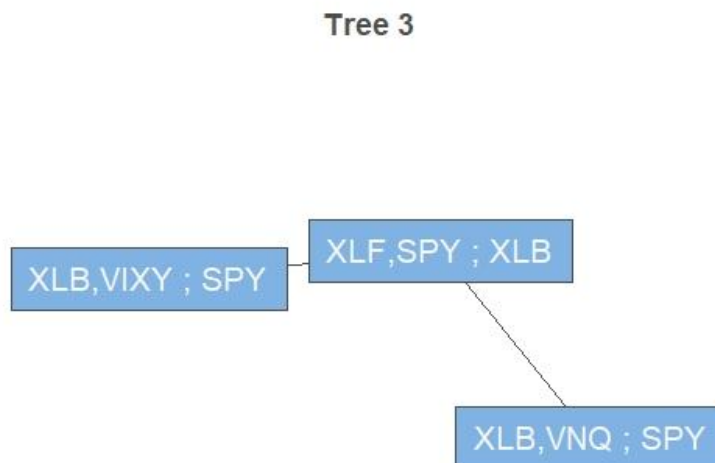


Figure 54: R-Vine Copula Conditional Dependence Tree (3)

Tree 4

Figure 55: R-Vine Copula Conditional Dependence Tree (4)

Plots for minimum variance portfolio weights

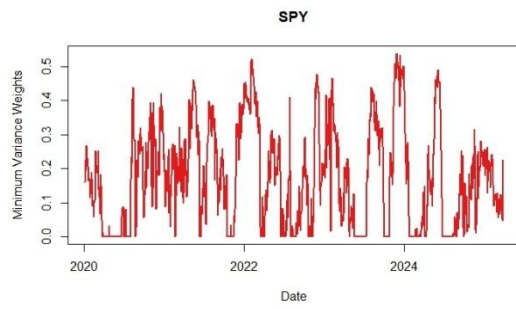


Figure 56: MVP weights SPY

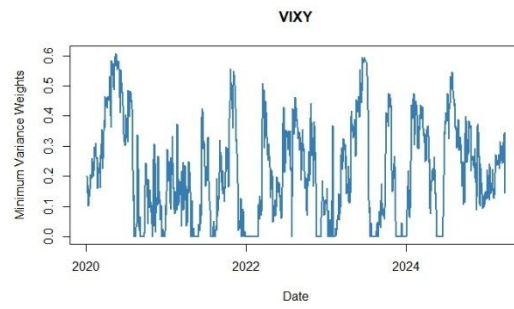


Figure 57: MVP weights VIXY

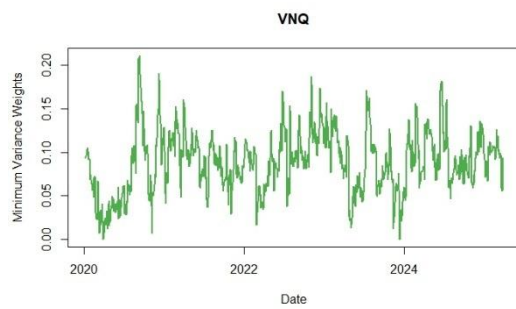


Figure 58: MVP weights VNQ

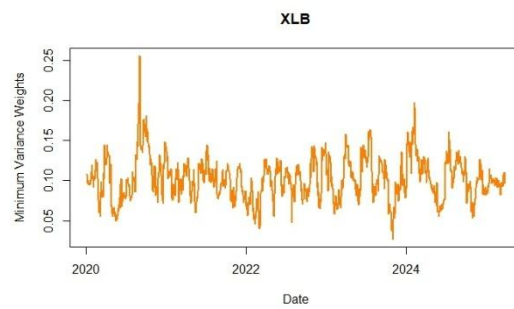


Figure 59: MVP weights XLB

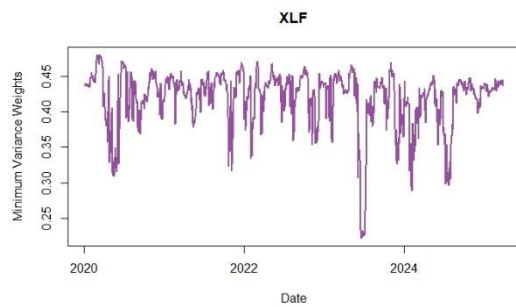


Figure 60: MVP weights XLF

Plots for minimum correlation portfolio weights

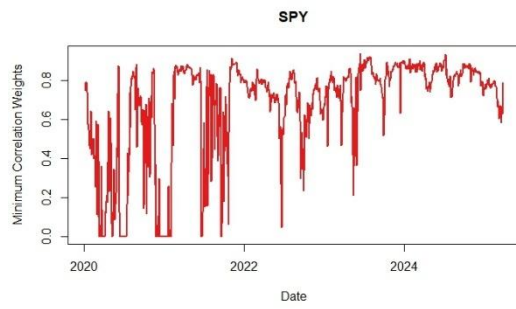


Figure 61: MCP weights SPY

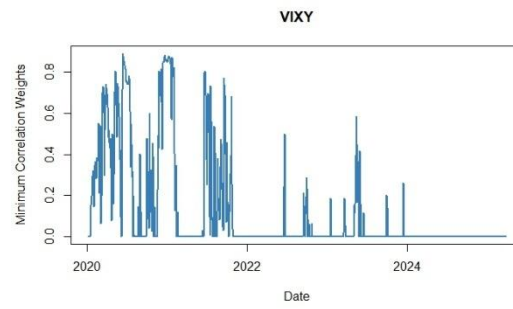


Figure 62: MCP weights VIXY

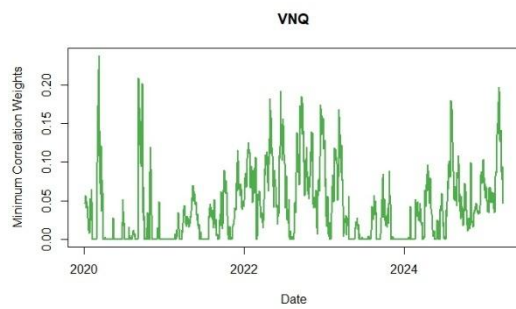


Figure 63: MCP weights VNQ

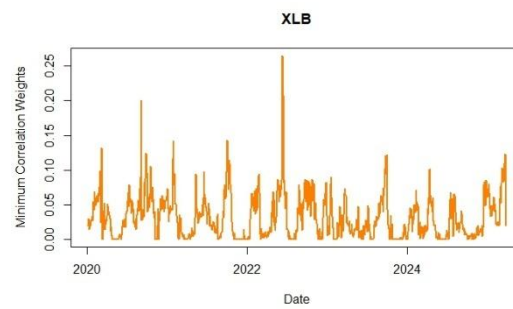


Figure 64: MCP weights XLB

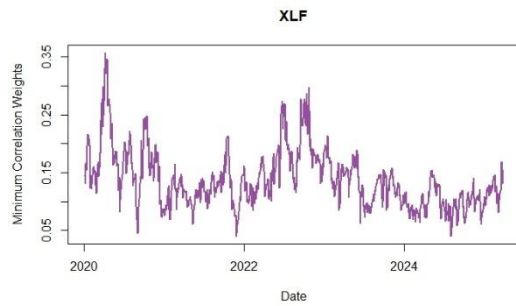


Figure 65: MCP weights XLF